NANOPARTICLE REINFORCED HYBRID COMPOSITE MATERIAL PRODUCTION PROCESS OPTIMIZATION

A MASTER'S THESIS

By

AZER DOĞUŞ KAÇMAZ

December 2017

NANOPARTICLE REINFORCED HYBRID COMPOSITE MATERIAL PRODUCTION PROCESS OPTIMIZATION

A THESIS
SUBMITTED TO THE DEPARTMENT OF MATERIALS SCIENCE AND
NANOTECHNOLOGY ENGINEERING
AND THE GRADUATE SCHOOL OF ENGINEERING & SCIENCE OF
ABDULLAH GUL UNIVERSITY
IN PARTIAL FULFILLMENT OF THE REQUIREMENTS
FOR THE DEGREE OF
MASTER OF SCIENCE

By
Azer Doğuş KAÇMAZ
December 2017

SCIENTIFIC ETHICS COMPLIANCE

I hereby declare that all information in this document has been obtained in accordance with academic rules and ethical conduct. I also declare that, as required by these rules and conduct, I have fully cited and referenced all materials and results that are not original to this work.

Azer Doğuş KAÇMAZ

REGULATORY COMPLIANCE

M.Sc. thesis titled **"NANOPARTICLE REINFORCED HYBRID COMPOSITE MATERIAL PRODUCTION PROCESS OPTIMIZATION"** has been prepared in accordance with the Thesis Writing Guidelines of the Abdullah Gül University, Graduate School of Engineering & Science.

Prepared By   Advisor

Azer Doğuş KAÇMAZ   Assist. Prof. Dr. Hatice Sinem ŞAŞ ÇAYCI

Head of the Materials Science and Nanotechnology Engineering

Prof. Dr. Murat DURANDURDU

ACCEPTANCE AND APPROVAL

M.Sc. thesis titled **"NANOPARTICLE REINFORCED HYBRID COMPOSITE MATERIAL PRODUCTION PROCESS OPTIMIZATION"** and prepared by Azer Doğuş Kaçmaz has been accepted by the jury in the Materials Science and Nanotechnology Engineering Graduate Program at Abdullah Gül University, Graduate School of Engineering & Science.

.... / 12 / 2017

JURY:

Assist. Prof. Dr. Hatice Sinem ŞAŞ ÇAYCI :…………………………….

Assoc. Prof. Dr. Mustafa Serdar GENÇ   :…………………………….

Assist. Prof. Dr. Cihan ÇİFTCİ   :…………………………….

APPROVAL:

The acceptance of this M.Sc. thesis has been approved by the decision of the Abdullah Gül University, Graduate School of Engineering & Science, Executive Board dated ….. /….. / ……….. and numbered …………..……. .

….. /….. / 2017

Graduate School Dean
Prof. Dr. İrfan ALAN

ABSTRACT

NANOPARTICLE REINFORCED HYBRID COMPOSITE MATERIAL PRODUCTION PROCESS OPTIMIZATION

Azer Doğuş Kaçmaz

MSc. in Materials Science and Nanotechnology Engineering

Supervisor: Assist. Prof. Dr. Hatice Sinem ŞAŞ ÇAYCI

December 2017

Composite materials have increasing application areas in today's industry and daily life due to their low density structure and high mechanical properties. Also, thermal stability and electrical conductivity can be improved by particle inclusion. Composite materials consist of preform, matrix and particles in matrix. Various production methods have been developed to bring these components together. Among these production methods, liquid composite molding methods are the most widely used methods for producing parts having advanced properties. A different method logic has been tried to obtain more homogeneous product than traditional resin Transfer Molding method in order to produce composite parts with superior mechanical properties. Since the Resin Transfer Molding (RTM) method is expensive and time-consuming, simulation is the fastest and economical method for optimization of the process. In this study, COMSOL software was used for numeric analysis. As a result, when production of hybrid composite materials with highly different permeable components performed with Resin Transfer Molding Method, Compression Resin Transfer Molding (CRTM) logic works much more precisely in terms of avoiding voids and providing homogeneity through preform when filling is performed from the top.

Keywords: Hybrid composite materials, Liquid Composite Molding, LCM, Resin Transfer Molding, RTM, Compression Resin Transfer Molding, CRTM

ÖZET

NANO-PARÇACIK TAKVİYELİ HİBRİT KOMPOZİT ÜRETİMİ İÇİN REÇİNE GEÇİŞLİ KALIPLAMA PROSESİ OPTİMİZASYONU

Azer Doğuş Kaçmaz

Malzeme Bilimi ve Nanoteknoloji Mühendisliği Bölümü Yüksek Lisans

Tez Yöneticisi: Yrd. Doç. Dr. Hatice Sinem ŞAŞ ÇAYCI

Aralık 2017

Kompozit malzemeler, düşük yoğunluklu yapıya ve yüksek mekanik özelliklere sahip olmanın yanısıra parçacık takviyesi ile iyileştirilebilen ısıl ve elektrik özellikleri sebebiyle günden güne artan uygulama alanlarına sahiptir. Kompozit malzemeler iskelet yapı, sıvı reçine ve reçine içerisinde parçacıklardan meydana gelmektedir. Bu bileşenleri bir araya getirmek için kullanılan üretim yöntemleri içerisinde sıvı transfer döküm methodları ileri seviyede özelliklere sahip parçalar üretmek için yaygın olarak kullanılmaktadır. Bu çalışmada üstün mekanik özelliklere sahip hibrid kompozit parçaların üretiminde istenilen homojen yapıyı elde etmek için reçine transfer döküm yöntemi değerlendirilmiştir. Bu yöntemin pahalı ekipmana ve uzun zamana ihtiyaç duyan bir yöntem olması sebebiyle iyileştirme sürecinde en hızlı ve ekonomik yöntem olan nümerik analiz yöntemi ve bunun için COMSOL yazılımı kullanılmıştır. Reçine transfer döküm yöntemi analiz edilirken, gözeneklilik fazrkı yüksek olan iki malzemeyi içeren kompozit malzemelerin üretiminin reçine transfer döküm metodu ile yapılması durumunda, ancak basınçlı reçine transfer mantığıyla dolum yapılması halinde homojen parça üretilebildiği sonucuna varılmıştır.

Anahtar kelimeler: Hibrid kompozitler, Reçine Transfer Döküm, Basınçlı Reçine Transfer Döküm

Acknowledgements

Table of Contents

List of Figures

List of Tables

Chapter 1

1 Introduction
1.1 Composite materials

Composite materials are the materials consisting two or more materials that are bonded each other and formed a continuous structure. Composite material technology started to be developed about 1960s. Their main structures and consisting materials are reinforcement material (porous or cracked structure such as glass, boron, carbon, etc.), resin (the liquid used to bond reinforcement structure), and particles in the liquid. Engineering significance of the composite materials arise from their light weight and high mechanical properties [1].

In the present day, human kind tries to meet their needs via various technological application adapted to the daily life. It is important using light materials having sufficient mechanical, physical and other needed properties. Weight becomes an important issue to solve for the industries due to its negative effect on fuel consumption and ease of use. Among them decreasing the effect of the spurring energy costs on the daily life without sacrificing from the performance has an essential role in automotive and aerospace industries. Due to common materials always have some disadvantages because of high operating costs, insufficient mechanical properties and high weight combinations. Therefore, economic and performance constraints force the scientists to searching for advanced materials with low weight, high mechanical properties, low maintenance and high corrosion resistance [2]. Figure 1.1a is about the increase of the composite material usage in BOEING air crafts over years and 1b gives the 787 Dreamliner's composite part percentage.
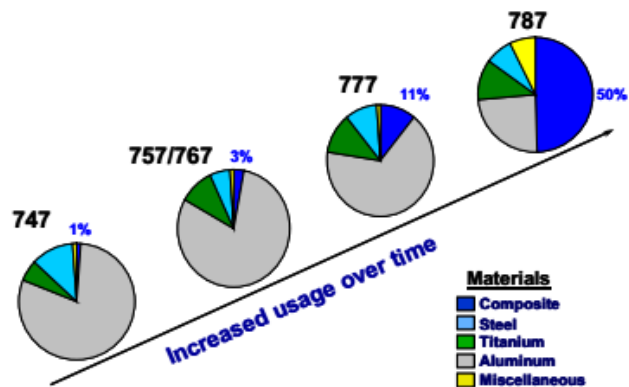
(a)
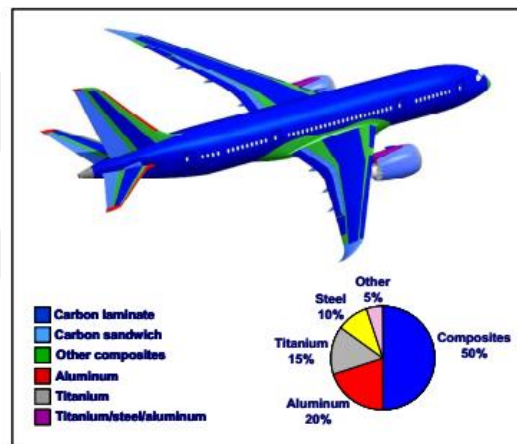
(b)

**Figure 1.1 (a) Composite Material Increase in Boeing Aircrafts over time
(b) Composite Material Percentage of the BOEING 787. [3]**

1.2 Composite Material Parts

Composite materials consisted of two main parts. These are resin and reinforcement parts. The resin is the liquid material which keeps the reinforcement material together while effecting various physical and mechanical properties if the composite materials. Reinforcement is the skeleton structure of the composite materials with various types determining main mechanical properties.

1.2.1 Reinforcement

Reinforcements role in the composite materials is the enhancing mechanical properties of the neat resin. These reinforcements can be synthetic fibers (glass, carbon, aramid, etc.), natural fibers (sisal, jute, cotton, etc.) and particles (clay, mica, titanium dioxide and so on) [3].

All these materials are stronger in fibrous form than bulk materials due to the high aspect ratio (length/diameter ratio) of fibrous form. High aspect ratio allows an effective load transfer system construction [4].

Synthetic fibers are commonly used in industrial applications. If needed to mention some of the prevalent synthetic fibers. Glass fibers are the one with less cost and high strength. However, glass fiber shows weak abrasion resistance which is undesired and reduces usability, strength and unwanted weak adhesive behavior when embedded in resin under moisture.

Among all reinforcement fibers, carbon fibers have the highest strength and stiffness. However, they are brittle than glass and may be effected from galvanic corrosion when used next to metals.

Aramid fibers are synthetic fibers having polymer form. Aramid fibers are not as brittle as glass or graphite fibers and have noteworthy tensile strength. Production of these fibers need much less heat, so they are more economical than glass or carbon fibers. However, these fibers have some disadvantages, for instance, Kevlar shows poor compression stability due to its anisotropic structure.

1.2.2 Matrix

Fibers cannot transmit forces individually due to their tiny cross-sectional areas. In order to make possible to bear loads with the fibers, it is essential to gather them. Embedding the fibers is possible via using a matrix material.

1.2.2.1 Polymeric Matrix

Polymeric matrices have two types that are thermosets (epoxy, polyester, polyimide) and thermoplastics (polyethylene, polystyrene, nylon, etc.). These matrices have moderate cost low density and easy processability.

Polymeric matrix materials also alter the mechanical properties of the fiber-reinforced composite materials, but their physical characteristics (melting temperature and viscosity) limits the service temperature (lower than the glass transition temperature) because of the change in the mechanical properties. Both thermosetting and thermoplastics can be used as a matrix.

Epoxy resin and polyester are most prevalent matrix materials. Also vinyl esters, polyimides, etc. can be mentioned as other polymeric matrixes.

1.2.2.2 Metallic Matrix

Metals have high mechanical properties, and they have high resistance to various severe environmental conditions including high temperature. Thus they come to an advantageous position against polymeric matrixes. However, they have disadvantages such as; high density, high chemical reactivity (with fibers and corrosion degrading the mechanical properties) when compared with polymeric matrices.

1.2.2.3 Ceramic Matrix

Ceramic matrix composites are lighter than metallic matrix composites and have higher strength and stiffness with better chemical and physical stability at high temperatures. Thus ceramic matrix composites are used in aerospace engine industry efficiently.

However, ceramics are highly vulnerable to the thermal shocks during the fabrication process and so porosity, a common flaw, which significantly degrades mechanical properties and increases unexpected failure possibility. Unfortunately, ceramics have low ductility relatively metal matrixes which makes

them brittle [5]. Ceramics have excellent friction properties in dry conditions, but they show a high response to humidity under cold and wet conditions that effects friction coefficient adversely [6]. Ceramic reinforced composite materials are costly materials due to their fabrication process at high temperature [4].

1.3 Fiber Reinforced Composites

Composite materials consist of resin (epoxy, polyester, vinyl ester, etc.) and reinforcement fibers (epoxy-glass, Kevlar, carbon fibers, etc.). Fibers are the discontinuous phase, and the matrix (resin) is the continuous phase of a composite material. Generally, matrix materials are softer and weaker than the reinforcement materials [4].

So, in composite materials resin bonds the fibers in it and protects them from the outside forces. Thus gathered fibers (preform) can stand higher stresses applied to the material which means this combination creates higher mechanical/physical/electrical properties [7–9] than their individual structures and substitutive materials.

It is possible to arrange the composite material properties by changing the fraction of resin/fiber combination [4,10,11] and orientation of the fibers [12] with controllable anisotropy [4]. Some most common orientations can be seen in Figure 1.2 [3].

The direction of the stress is an important issue, and stress with a changing direction is a hard situation to handle in a long time working period of the material. Fortunately, composite materials' direction of the strength can be determined during the fabrication process. Reinforcement fibers are the structures resist against forces, and it is possible to orientate them in any direction and needed concentrations to fabricate composite materials having desired mechanical properties [1]. In Figure 1.3 tensile strength and fiber orientation angle relation are shown.
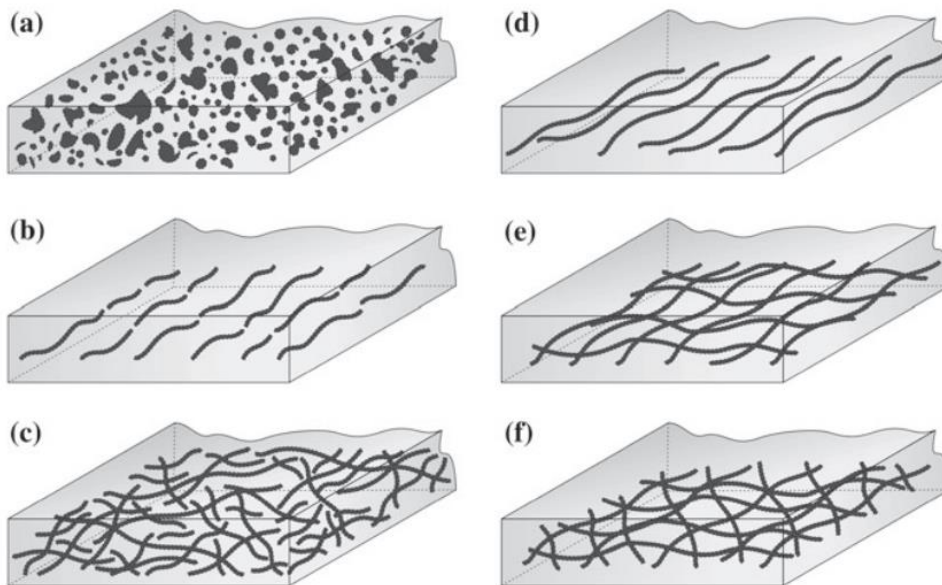
Figure 1.2 Classification and types of composite materials. (a) Dispersed particle-reinforced, (b) Discontinuous fiber reinforced (aligned), (c) Discontinuous fiber reinforced (randomly oriented), (d) Continuous fiber reinforced (aligned), (e) Fiber reinforced [3]
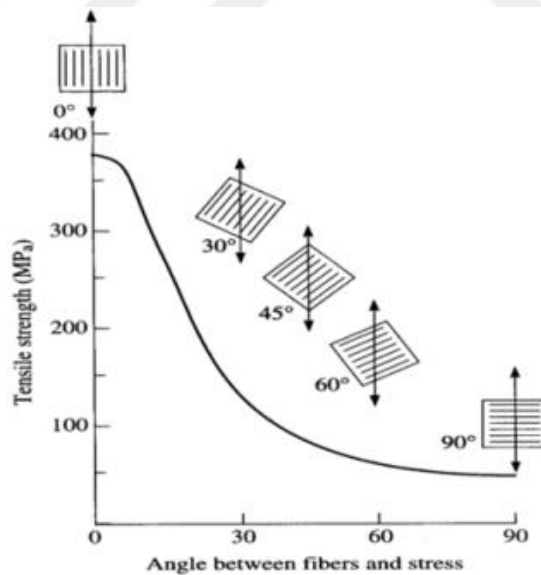
Figure 1.3 Fiber Angle and Tensile Strength Relation [14]

Also, resin and fiber interactions can be effective on mechanical properties. If the adhesive relation between matrix and resin increases alkali condition of the environment becomes dominant. Alkali-treated fibers result in better tensile

strength than untreated ones, as observed from the research of rubber resin –sisal and oil palm fibers composites [13].

Composite materials have a lower weight than the materials with similar or close properties. Thus, composite materials have a wide range of usage in various areas such as; automotive, aerospace, marine, medical, sports good industries, etc. [2,8,12].

Reinforcement fiber must form a structure in the composite material to satisfy mechanical needs, and some other factors such as; processability, feasibility of the geometry and cost of production are must be taken into consideration while determining the reinforcement geometry. Preforms may have continuous and discontinuous fiber alignment and two types of preform forms; weaving yarns and rovings [14]. Orientating the fibers in a structure which is a significant advantage when designing. In Figure 1.4 common fiber reinforcement structures are indicated [5].
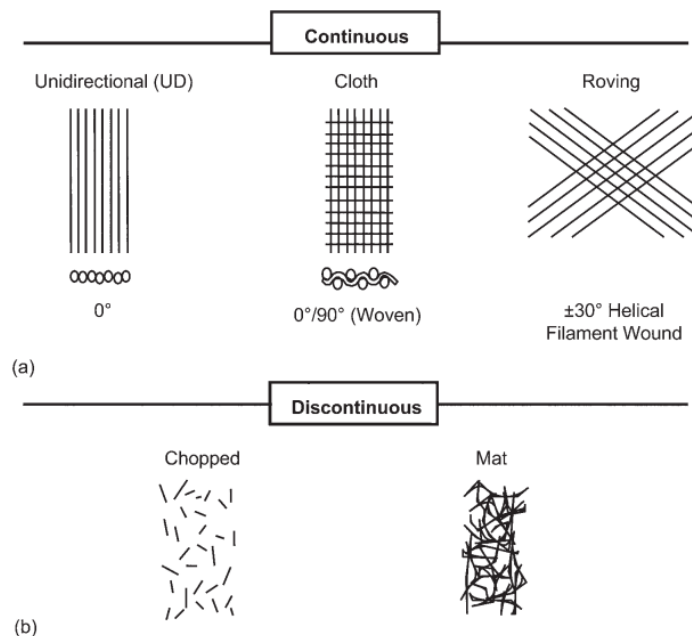
Figure 1.4 Typical Reinforcement Structural Types [5]

1.4 Hybrid Composite Materials

Hybrid composite materials are the ones consisting of two or more different fibers. Hybridization can be realized by using two methods. The first method is mixing the fibers deeply each other before depositing them into the same matrix. The second method is different types of fibers placed layer by layer individually, and orientation of these plies make possible controlling the anisotropy [4].

The general idea behind the hybrid composites is the production of relatively low-cost composites with high mechanical characteristics (tensile strength, impact energy) depending on requirements. For instance, the aerospace industry needs hybrid composite materials due to the need of specified materials with high impact energy and high modulus/weight ratio. In Figure 1.5 an example of how adding different fibers increase impact energy of composite materials [4].
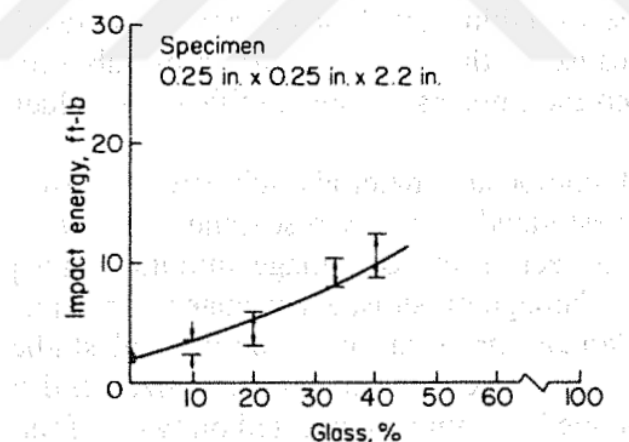
Figure 1.5 Influence of Adding Glass Fibers in a Graphite-Epoxy Laminate regarding Impact Energy [4]

It is possible to make a combination of any fiber types like synthetic-synthetic, natural-synthetic, synthetic-metal and all fiber types have different properties and costs. Thus it is possible to meet desired mechanical specifications with relatively low production costs. However, hybrid composite manufacturing needs an optimized combination of materials which is a challenge to be handled [15,16].

Hybrid composite material combination determined with the help of several tries and tests. Thus, increase in material and time consumptions is inevitable.

1.4.1 Particle Inclusions

In hybrid composites, some fillers (calcium carbonate, silica, cotton, natural fibers, nano-clays, SiC, CNTs, etc.) are used as inclusions to reduce the cost, control viscosity and obtain partial stiffness of composite at macro scale. Also, characterizing phonons, aspect ratios, thickness, particle shape (hollow, spherical, fiber, etc.) at nano-scale effect the thermal, electrical properties and elasticity of hybrid composite [17–19]. These fillers are generally micro and nano-sized materials improving fire resistance (e.g., antimony oxide), electrical insulation – thermal conductivity and dimensional stability (e.g., natural silica) are some of the benefits of the fillers.

Micro-sized fillers may be at high volume contents which are lower than volume packing factor to obtain desired thermal properties but reduce mechanical properties at macro level [18]. Similarly, nano sized fillers improve the physical and mechanical properties at low content rates (< 5wt. %) oppositely high content rates [20] because high nano sized filler content nano reduce physical and mechanical properties of composite materials due to high surface energy of nanoparticles which lead to form clusters and do not transfer their superior mechanical and physical properties to the matrix. Thus, dispersion of these particles must be performed particularly [21–23]. Also, high filler content ends up with an increase in resin viscosities [24] at inappropriate rates complicating production process and result in inhomogeneous dispersion of filler content due to microscopic cake filtration. Thus, in order to control all aforementioned effects, amount and shape of the fillers is an important subject to be determined precisely [17,18,25].

Nano-crystal materials have high strength and have corrosion and wear resistance at high temperatures that is why in composite materials nano-scaled materials are used for better mechanical properties. Additionally, nano-scaled particles infused

in the matrix may fill the voids in the composite material, and high surface energy of nanoparticles improves the crosslinking in the matrix which makes nano-sized particles superior to micron-sized ones. [20].

Nano-sized SiC particles may be used to improve thermal stability [20], CNTs inclusions tend to improve electrical properties [17].

1.5 Composite Material Manufacturing

Composite materials consist of two or more materials. In order to get these different materials Lay-Up, Spray-Up, Filament Winding, Pultrusion and Liquid Composite Molding (LCM) processes are the most common methods of composite fabrication.

All of these methods have similar issues to be handled. These are; production quality (surface quality, homogeneity, flaws, etc.), cycle time, dimensional stability, capability of producing complex parts, preform deformation rate (compaction pressure) and compatibility with production materials (fiber volume fraction, resin type, etc.).

LCM is a way of manufacturing composite materials by injection a liquid resin into a fibrous structure. The part geometry can be complex in aerospace and automotive industries which make LCM method preferable to the other methods due to its advantage of getting net shapes. Also, LCM has less manufacturing cost and higher performance among them [9,26,27].

LCM processes include Resin Transfer Molding (RTM), Vacuum Assisted Resin Transfer Molding (VARTM), Seeman Composite Resin Infusion Molding (SCRIMP), Structural Reaction Injection Molding (SRIM), Compression Resin Transfer Molding (CRTM) [2,27]. RTM and CRTM which are the two types of the LCM methods are shown in Figure 1.6.
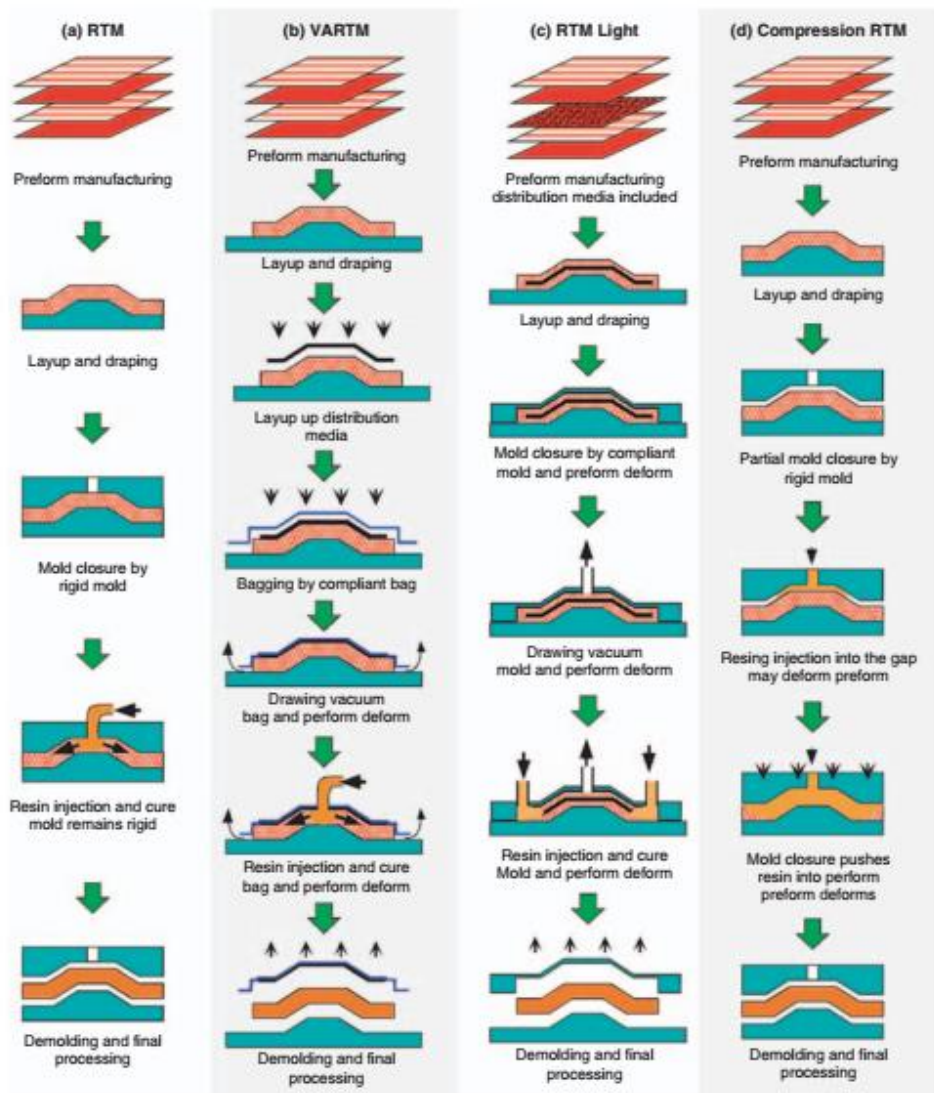
Figure 1.6 The Most Common LCM Processes [2]

The oldest fabrication technique is the hand lay-up method. Spray lay-up method is a semi-automated hand lay-up method. These are low-cost techniques and easy. Large and complex parts can be fabricated by these techniques. It is possible to produce large parts and system highly flexible but when high volume production is needed these methods do not meet feasible manufacturing time. Another disadvantage of these methods is standardization of material quality because of their dependency on operator talent.

Another method is Filament Winding method. During filament winding process reinforcement fibers, firstly pulled from the fiber rovings, and then goes in to a

resin bath and lastly wound over a mandrel so it is used to produce circularly shaped surfaces like tubes, cylinders, etc. This method allows automated high volume productions and dimensional flexibility in material design. However, it is difficult winding at low angles (parallel to mandrane) and obtaining double curvative shapes, so fabrication talent at desired mechanical properties and surface quality of the final product is relatively poor.

Additionally, Pultrusion is a technique have been used composite material fabrication. Pultrusion is convenient for high fiber volume materials with various shapes. However, pulturison machines are most suitable for thermosetting resins so; thermoplastic resins cannot be used without equipment modification.

1.5.1 Resin Transfer Molding (RTM) Process

RTM has recently become one of the common composite material production methods. RTM process consists of three phases: 1- Rigid mold preparation with fiber beds, 2- Resin impregnation and 3- Curing. In the first step fiber layer are aligned in the mold which is rigid and closed (except at least one apiece resin inlet gate and outlet-air discharge gate) during the filling process. Then wetting process starts and low viscous resin impregnates into the mold with the help of the pressure difference created by the pressure pump, and the air is discharged. During the impregnation process, thermoset resin flow at constant pressure or constant flow rate. Figure 1.7 shows the impregnation of the melted resin through reinforcement (porous media) and in Figure 1.8 impregnation process at different times is visualized.
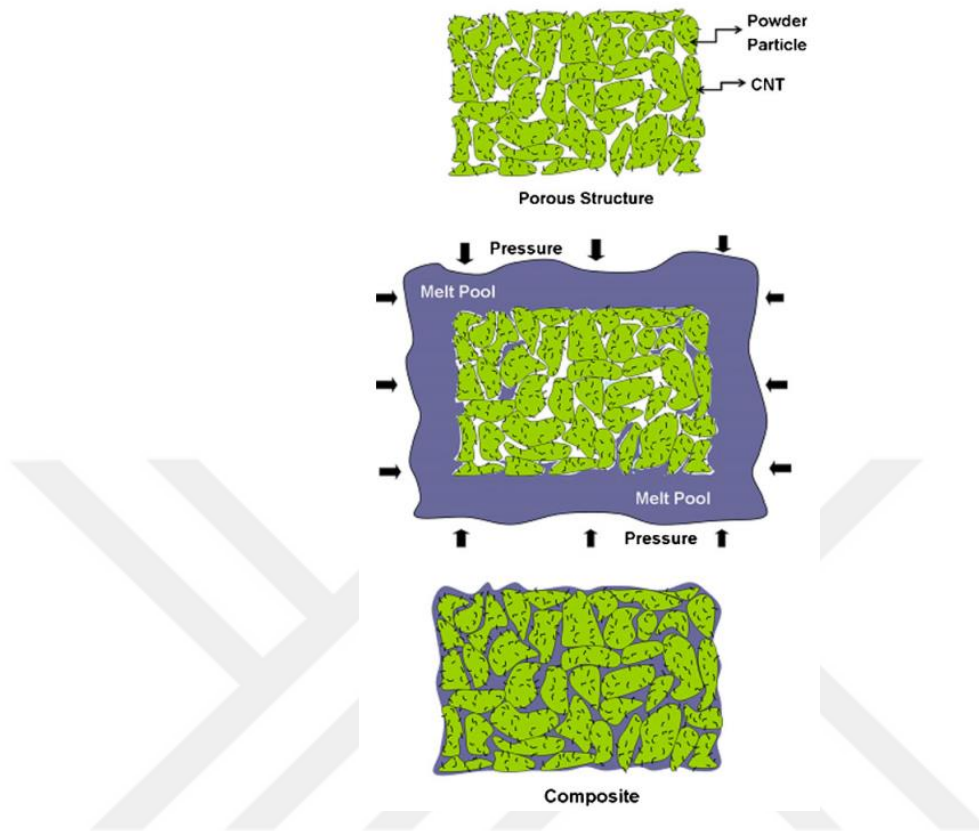
Figure 1.7 Impregnation of Melt Resin Through Porous Structure [28]
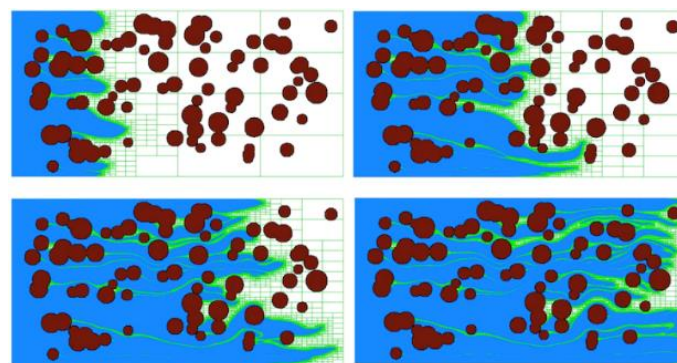
Figure 1.8 Simulation of The Flow Through Porous Media at Different Times [29]

As resin flows through the fibrous preform, cross-linking starts between polymers which can be called pre-curing. Lastly molded material cured with the heat

treatment which finishes the consolidation and cross-linking [2,30,31]. In Figure 1.9 whole RTM fabrication cycle is shown.
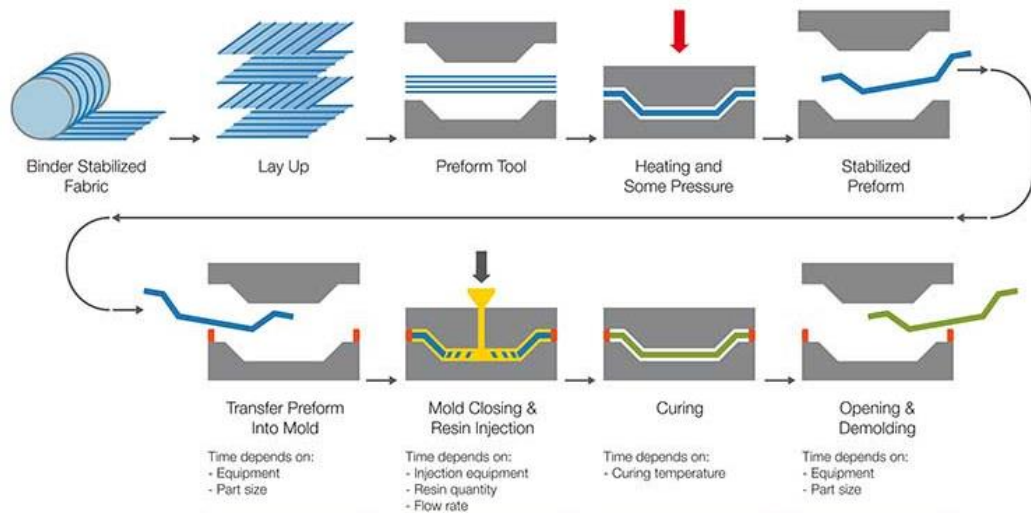
Figure 1.7 Resin Transfer Molding Cycle [32]

Through the end of impregnation phase, compaction phase can occur. In compaction phase, pressure in the rigid mold may increase as the preform is saturated. This phenomenon can be considered as an external force which may form new fiber arrangement and permanent change in microstructure like nesting. Unfortunately, all these may lead to alter failure mechanics characteristic and permeability of composite material [14] so it is essential to prevent compaction phase as early as possible.

With RTM process large continuous fiber reinforced composite materials can be fabricated in relatively short time cycles. Orientation of fibers are more controllable in RTM method so the mechanical properties of composites [4].

RTM method has some more advantages over the other production methods. Some of them are the dimensional stability which enables to work with small tolerances, getting a good surface quality and thickness control [2]. Also, RTM

needs relatively low pressure to keep the mold closed. Furthermore, RTM has relatively short cycle time so it is very convenient for high volume productions (between 100 – 10.000 parts) and it provides a better control on mechanical properties [32]. The advantage of getting net shape product from the RTM method eases repetitive fabrication of complicated part easier than the other methods. However, RTM method has some disadvantages. In large part production front flow velocity decrease is unavoidable and results in longer filling times. In order to speed up filling rate inlet pressure can be increased but the front flow with high pressure can result in mold or preform deformation. Also, heating the resin or system to lower the flow viscosity may start gelatinization of resin earlier [33]. RTM equipment is expensive, and optimization of the parameters should be done precisely.

1.5.2 Compression Resin Transfer Molding (CRTM)

One of the prevalent variations of the RTM is Compression Resin Transfer Molding at which an external force is applied to dynamic mold after the injection process. The first stage is the injection of the resin to the pattern in the mold and at this stage, preform deforms very slightly unlike VARTM. The space between mold wall and the preform is filled with resin, and then compression starts. The motion of the mold closes the gap and pushes the resin into the fibrous media with constant force. Thus injected resin between the movable mold and the preform, impregnates to the fibrous media. When the movable space closed process finishes. CRTM has a more wettability capacity of fibers over RTM process.

As the fiber volume fraction increases local permeability decreases and filling time gets longer. Thus, injection process requires higher injection pressure that may cause increase the possibility of void formation and the probability of structural deformation due to increased flow velocity and pressure. [33,34] result in cost increase. Compression of CRTM method allows high fiber volume fraction fabrication with faster filling time unlike RTM method [35]. However,

compaction phenomena must be kept in mind as in RTM [36] due to high pressure need and inhomogeneous particle distribution near vertical lines.

1.5.3 Vacuum Assisted Resin Transfer Molding (VARTM)

VARTM is another method used to fabricate composite materials with fibrous reinforcement and particle added resin [37]. In this method, multiple fibrous layers are placed and packed in a mold where resin flows through the preform. In VARTM production flow media covered with a plastic bag or elastic membrane, which is vacuumed by a vacuum pump. This pressure difference makes resin flow through the fibrous media layers and starts impregnation [38]. In Figure 1.8 an example for VARTM process equipment is shown.

**Figure 1.8 Detail of VARTM Process. 1- Vacuum Pump, 2- Safety Tank, 3-
Indicator, 4- Distribution Layer, 5- Dacron Peel Ply, 6- Vacuum Bag, 7-
Resin Transfer Tube, 8- Valves and Joints, 9- Release Wax, 10- Seal Paste
[40]**

VARTM differs in the pressure difference created by a vacuum pump between the inlet and outlet because vacuum degree is responsible from the amount of air entrapped in the pores which cause defects and degrades the mechanical properties of composite material [25].

VARTM method allows manufacturing of large parts with high fiber volume fraction relatively low cost. Although VARI has less tooling costs than RTM, in

VARI deformation of the elastic cover of the fibrous media during injection should be taken into account during production and modeling processes [26].

1.5.4 SEEMAN Composite Resin Infusion Molding Process (SCRIMP)

SCRIMP method is very similar to VARTM method. As in VARTM process resin flows first into the free channel and then through porous media with the help of vacuum in SCRIMP [39]. Before resin flow starts, fibers are compacted that reduces void formation and increases fiber percentage. Also, a patented layer is used for resin distribution along the layer. Advantages of this method are its' capability of producing high fiber content composite materials, decreasing void forming probability [40]. A schematic illustration of SCRIMP is shown in Figure 1.9 [41].
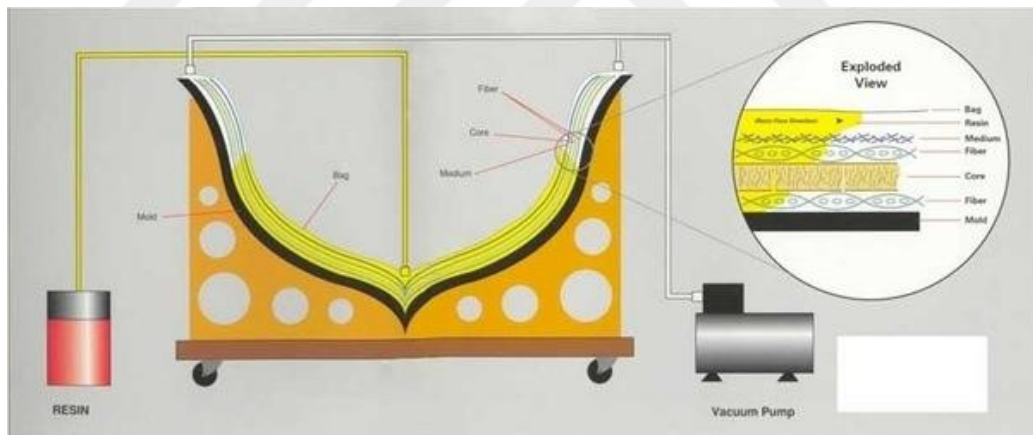
Figure 1.9 A Schematic Illustration of SCRIMP Process

In this method one side of the preform is mold, and the other side is vacuum bag which reduces the tool cost [42] and it is possible to fabricate large parts with complex geometries [39]. However, the resin must have a very low viscosity, so its' mechanical properties, relatively complex application and some elements are protected by patents and expensive to license.

1.5.5 Challenges in LCM

There are several challenges to be handled during choosing LCM method and LCM production processes. A preliminary issue is determining the LCM type. Choosing the method for production depends on the several variables such as; cycle time, need of experienced staff, cost of equipment, the complexity of part shape, production quality (surface smoothness, fully filled geometry) and compatibility with the material (porosity of reinforcement, the viscosity of resin) to be used. Also, in especially RTM methods effected from injection rate, inlet/outlet gate position, size and number (filling time, hardening time, avoiding voids), fiber volume fraction (capability of RTM method), flow rate or inlet pressure/vacuum rate (void formation rate), reinforcement stability (compaction phenomena), temperature and complexity of geometry to get desired cycle time, homogeneity and mechanical properties.

1.5.6 Challenges in Lcm with Hybrid Composites

Hybrid composite material production has some more subjects to be considered. As mentioned above hybrid composites include nano and micro-sized particles. The amount, size and shape of these particles affect various properties of the composite material, and it is essential obtaining a homogeneous dispersion of these particles. Additionally, high amount of particles results in a high viscosity of the resin, and this is an important subject in the production process. Even though high-temperature rate lowers resin viscosity, gelatinization becomes an issue to be considered.

1.6 Scope and Objective of Thesis

This thesis focuses on the processing of hybrid composite materials with micron scale particles by Resin Transfer Molding method at macro level to produce a homogeneous hybrid composite material via understanding behaviors and interactions of various process parameters such as; fiber reinforcement porosity, resin viscosity, flow front velocity, inlet and outlet gate orientations, geometry,

injection pressure, filling time and particle concentration. Mentioned parameters effect homogeneity of produced composite part, the formation of voids, particle distribution and so the mechanical properties of the hybrid composite materials. Firstly, the mathematical model constructed as a combination of models constructed by Erdal [43] and Lefevre [44] with capillary pressure add. The model defines the flow of the Newtonian fluid through the porous medium. A study conducted at macro-level, so Darcy Law is used for incompressible flow investigation. Permeability is defined by Lefevre's [44] definition including Kozeny Carman relationship. Inertial effects, cake filtration, and temperature effect are ignored. Then with the help of this mathematical model numerical simulation via COMSOL Multiphysics$^{©}$ is conducted.

In chapter 1, information about composite materials, hybrid composite materials, their consisting parts (matrix reinforcement and particles), composite material production methods, Resin Transfer Molding, Compressing Resin Transfer Molding, Vacuum Assisted Resin Transfer Molding, Seeman Composite Resin Infusion Molding and challenges of these processes are introduced.

In chapter 2, reasons behind the need for numerical modeling are discussed. Numerical model approaches in the literature are presented.

Chapter 3 includes explanations of mathematical variables belonging to RTM process and constructed mathematical model via approaches in the literature.

In chapter 4, COMSOL Multiphysics$^{©}$ simulation is explained particularly. Optimizations are explained and results presented.

Finally, a summary of main results of the study and outlook for future works are presented in chapter 5.

Chapter 2

2 Modelling of RTM

2.1 Need for Numerical Modelling of RTM

RTM is a low-pressure process, and resin has high viscosity, but the possibility of defected fabrication is not zero. Even though the flow of the resin velocity is slow and inlet pressure is higher than the outlet some unfilled parts and non-uniform distribution of the resin is observed especially when complicated parts are the subject.

RTM fabrication is an expensive method due to the equipment cost and production time cost. Although RTM is a low-pressure process it is critical optimizing interdependent RTM parameters such as; flow rate, inlet pressure rate, temperature, inlet and outlet gate orientation, viscosity, permeability filling time, and volume fraction [14,32,45–48]. Thus RTM process mostly consists of experience, trial and error procedures which are often time expensive and costly because of modification of the mold and repeating the trials are the realization of several configurations including all the parameters mentioned above with the excessive raw material consumption.

As mentioned above RTM process can be performed with constant flow rate and constant inlet pressure [49] as shown in the Fıgure 2.1, Masoodi and his friends [27] experiment represents that tracking the front-flow is very precise when injection at constant flow rate unlikely constant inlet pressure injection.
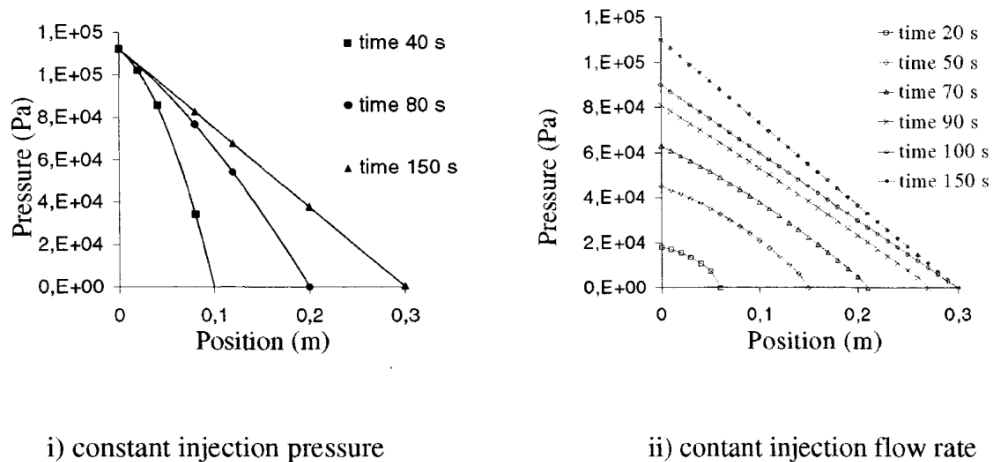
Figure 2.1 Comparison of Pressure Drop at Constant Injection Pressure and Constant Flow Rate [49]

Lin and friends [46] described various optimization methods like quasi-Newton and gradient-based methods for optimization of various dependent variables each other and their FEM analysis gives a solution of how to find the optimal gate numbers and positions without sacrificing the quality. The optimization of the gate positions is shown in Figure 2.2 to obtain the shortest cycle time.

Initial gate locations   Final gate locations

0.1 m
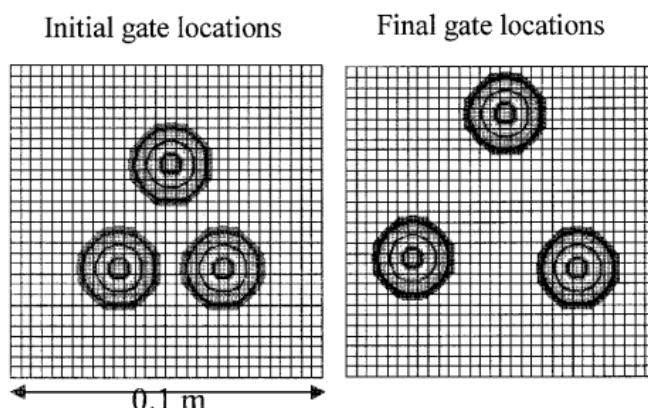
Figure 2.2 Gate Locations Before and After The Optimization [46]

Simacek and friends [2] conducted a study about the how number, spacing and the positions of the folds affect the resin distribution in the mold. This study shows that not only the optimum injection pressure and the number of the gates is

enough, but also the spacing of the gates should be analyzed considering the relation between all to fabricate flawless complex parts.

Bréard and friend's study [49] shows that front flow velocity has a great effect on the saturation of the unsaturated preform. Also, there are other studies proved flow characteristic effect upon the void formation. Reach angle and velocity of resin flow are some values depending on the flow characteristic. It is proposed that capillary number should be equal or below of critical capillary number, which is a function of front flow velocity, resin viscosity, and surface tension because over the critical capillary number void formation increase exponentially [26,50,51]. The mechanism of void formation is illustrated in Figure 2.3.
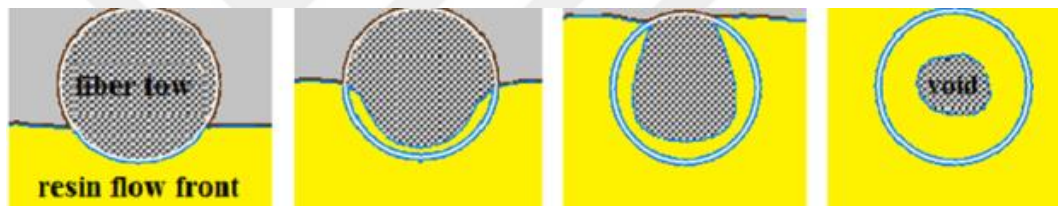
Figure 2.3 Void Formation Mechanism in the Intra-Bundle [14]

Formed voids during the RTM process worsens the mechanical properties and surface quality of the composite material [52,53]. Thus it is essential to avoid the void formation in the composite material in order to meet the desired mechanical and surface properties. Therefore, RTM process should be simulated for optimization to reduce void formation possibility [31]. So it is essential to obtain a saturated flow during injection as presented in Figure 2.4.
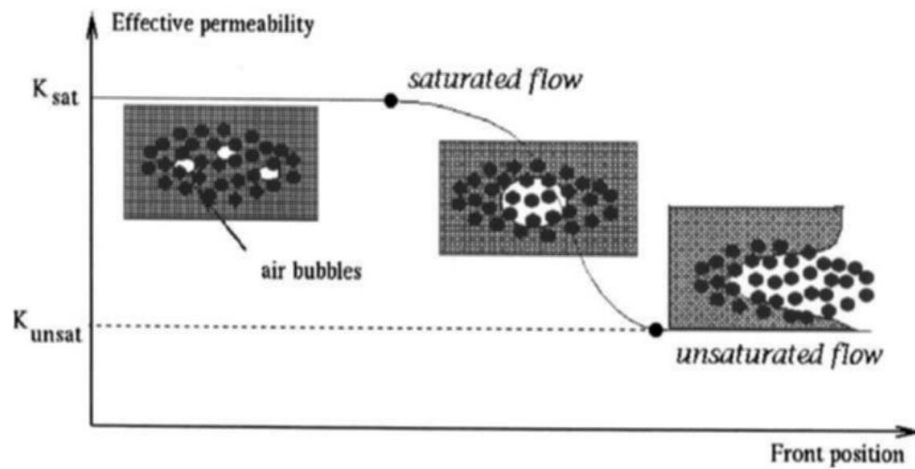
Figure 2.4 Difference Between Saturated And Unsaturated Flow [49]

Ruiz and friends conducted a study about the relationship between injection flow rates/injection pressure and void formation in RTM process. During this analysis, capillary number calculated and then injection rate is corrected until the optimum flow rate with a capillary number below the critical capillary value is found to decrease the void formation.

The most cost-effective and fast way of optimization of RTM process is finite element simulation. PORE-FLOW[©], RTMFLOT[©], CRIMSON[©], PAM-RTM[©], MOLDFLOW[©], LIMS[©] [27] and ANSYS[©], ABAQUS[©] (with some restrictions) [45], FORTRAN[©] [54], Star-CCM[©], COMSOL Multiphysics[©] [55] are the software which may be used for RTM simulation.

2.2 Numerical Approaches

There are several FEM analyses carried out about the particle filtration and flow through the 1-D, 2-D, 3-D porous media. These simulations are conducted to observe flow front position at several times and resin distribution during the injection. Also, it is possible to detect the resin impregnation, clogging and particle filtration rates at different orientations. Simulation gives the opportunity changing the LCM parameters like porosity, flow rate, inject pressure, permeability, particle size, resin concentration and gate positions, etc.

Lefevre and colleagues [44] they used Mat lab and COMSOL$^{©}$ to simulate an LCM process. They defined some input parameters depending on the geometry (length), material (porosity, permeability, viscosity) and technological capabilities (injection pressure). The model mainly based on 1-D Darcy law and power law viscosity definitions. In this model permeability and viscosity values are not constant and updates with time and position due to retention phenomenon. They proposed that retention has the highest value at the inlet and so permeability has the lowest value. Porosity change with time pointed to the clogging during the injection. This simulation conducted for three different particle concentrations and study resulted in high concentration particle causes higher retention rates and longer filling times.

Some numerical analysis conducted to find out the relation between inlet velocity and void percentage. Results show that when resin inlet velocity causes capillary number pass the critical value, larger void areas are observed. The simulation once calculates the capillary number, and if it exceeds the critical value, it corrects the inlet flow rate. This optimized flow velocity gives the shortest filling time with minimum void areas [26,31].

A CRTM for complex part fabrication is simulated in LIMS$^{©}$ by Simacek and colleagues [2]. They proposed that the gap between the injection points effects the saturation of the preform. As the gaps are pointed closer, the saturated area is larger at a time. Also, they observed that at a constant flow rate larger gap system has higher pressure increase at the inlet which is dramatically high from the small gap sized filling system.

Another paper is about Stoke/Darcy coupled flow in porous media. A 2-D FORTRAN$^{©}$ code is written and geometry contains a free flow channel, and a porous media engaged from the middle of the free flow channel. Simulations carried out between 10^{-6}-10^{-12} m^2 porosity values. They observed that in their geometry, porous media with low permeability results in less flow through the porous media [54].

Particle distribution is also a subject to be analyzed. A Darcy Law approach for dual scale porous medium VARTM model is used to analyze the filtration phenomenon and so the distribution of the particles through the preform. 6 layers woven dual scale fibrous media consist some macro-pores in the middle of four fiber intersection square. Simulation model results give that 60% of the particles deposited in the first layer and model carried out for different particle sizes (10-80 μm) with constant volume fraction. Sturdy shows that small particles distribute more uniform than big particles. Also, any smaller particles than macro pores give an even distribution through the preform layers. This study proposes that particle distribution is dependent on particle size distribution which is affiliated with the architecture and the pore size profile of the layers [38].

Masoodi and colleagues [27] used PORE-FLOW$^{©}$ software for simulating LCM process through a natural fiber preform. This simulation conducted with the mathematics Darcy Law, Kozeny Carman permeability expression. Two conditions, constant inlet pressure and constant inlet velocity are tried. It is found out that flow front position can be tracked very well under the conditions of the constant flow rate. Major finding of this study is the swelling of the wetted natural fibers effects on permeability. Due to change in the fiber dimensions, using a time-dependent permeability function becomes compulsory.

One more study is about the determination of permeability in single and dual scale permeability via ANSYS$^{©}$ software. Although ANSYS$^{©}$ allows work on various mold shapes, it is hard to engage influence of temperature, and concentration estimation is needed. Simulation performed in order to determine the best gate orientation and flow rate aiming to obtain homogeny distribution of the resin in the porous media because inhomogeneity results in composite materials with undesired mechanical properties. As a result, when the incompressible high viscosity is the subject, it is stated that with high Re numbers Forcheimmer's law should be taken into account instead of Darcy Law for macro level analysis [45].

Also, some models are constructed to determine the pressure drop and its' reasons during injection. The fiber pattern orientation and fiber diameter determined as the main variables affect the pressure drop due to change in porosity [32].

Another numeric model is carried out to predict filler retention profile and cake filtration profile (cake filtration form when the particle size is bigger than pore size). It is found out that as the filler particle concentration increases at the filter cake which located at the ahead of fibrous medium), the pressure drop increases at constant flow rate. Additionally, retention has the highest value at the entrance and the lowest at the exit of the cake, so the porosity profile (related to compression of the cake with an exponentially decreasing profile through the end of the cake) is vice versa [56].

A numerical tool study with the level-set method is conducted to evaluate the particle deposition at mesoscale. Flow in dual scale porous media is described by the Stokes–Brinkman coupling. It is proposed that permeability value and deposition rate have a direct relationship and the most particle deposition observed in the middle of the central fiber tow at where fluid velocity is very small. Fluid velocity gets faster at the neighboring regions due to blocking the effect of already deposited particles which reduces local permeability resulting in particle deposition nearby regions [37].

Erdal and colleagues [43] conducted a study on impregnation molding of ceramics. Darcy Law flow, Kozeny-Carman permeability relation, and Mentzer viscosity definition are used for analysis. It is observed that process parameters (injection velocity, inlet particle concentration, preform volume fraction, permeability, initial filtration coefficient and resin viscosity) are nonlinearly interdependent. Should be noted that anisotropy of the flow domain, filler particle size, and distribution, of preform pore geometry parameters are ignored. It is the proposed that porosity increase of preform at constant permeability initial filtration coefficient increases due to increase in the specific surface of the preform. Although it is possible to keep the permeability constant while

determining the initial filtration coefficient permeability rate has a relationship with particle distribution profile. Permeability has the lowest value at the inlet due to the accumulation of the particles and vice versa at the outlet, so inlet particle concentration becomes important for the local permeability value through the flow. Additionally, results show that injection flow rate does not alter the particle distribution profile so and so the permeability. The preform geometry is changed by varying fiber volume fraction, and the preform permeability and the highest variation of particle distribution are observed at the highest fiber volume fraction. As a result of this study, impregnation process design can be achieved by considering these mentioned parameters to obtain a process with less cycle leading to a cost-effective fabrication.

2.3 Need for Mathematical Model and Approaches

Resin transfer molding process has distinctive physical mechanisms and parameters of these. These parameters are like permeability, retention, porosity, filtration, pressure drop, mass flow rate, etc. All these parameters interact each other thus, determining physics behind them and relationships of these variables is a critical work for both understanding the phenomena and optimization of system and mathematical models can identify the RTM process in an effective way. There are several studies in the literature on both mathematical model construction particles filled resin flow through a dual scale porous medium in macro scale and simulations of these models.

Leferve et al. [44] conducted a simulation study and constructed a mathematical model for this simulation. Flow investigated at macro level under constant injection and also resin fluid shows non-Newtonian behavior. (Darcy Law Eq.2.3.1) is used to define the momentum equation through porous media.

$$U = \varepsilon * v = -\frac{K}{\mu}\Delta P \qquad \text{Eq. [2.3.1]}$$

A filtration sub-model is used including porosity (ε) (Eq. 2.3.2), a variable of entrapped liquid between retained particles (σ) (Eq. 2.3.3).

$$\varepsilon = \varepsilon_0 - \beta\sigma \qquad\qquad \text{Eq. [2.3.2]}$$

$$\beta = \beta_0 - r\sigma \qquad\qquad \text{Eq. [2.3.3]}$$

Mass balance equation is defined (Eq. 2.3.4) with no diffusion and no physico-chemical interaction as a constitutive equation.

$$\varepsilon\frac{\partial C}{\partial t} + U\frac{\partial C}{\partial x} = (\beta_0 C - 2rC\sigma - 1)\frac{\partial \sigma}{\partial t} \qquad\qquad \text{Eq. [2.3.4]}$$

A particle deposition kinetic equation is also defined (Eq. 2.3.5). In that equation k_0 is initial filtration coefficient. Deposited particles' re-suspension is ignored.

$$\frac{\partial \sigma}{\partial t} = k_0 UC \qquad\qquad \text{Eq. [2.3.5]}$$

The resin fluid shows non-Newtonian behavior so shear-stress has to be taken into consideration. Thus power law viscosity formula is used for viscosity definition (Eq. 2.3.6) including average shear rate (γ) at which m is an experimental constant and n is a variable as a function of initial resin concentration.

$$\mu = m\gamma^{n-1} \qquad\qquad \text{Eq. [2.3.6]}$$

Permeability also defined as a function of fiber preform related permeability (K_{fiber}) and deposit particle related permeability, K_d, with perfect saturation assumption of system. Then permeability calculated as average of them as two

parallel systems. Definition of retained particle permeability is estimated via Kozeny-Carman relationship (Eq. 2.3.7) and over all permeability calculation is defined as equation 2.3.8.

$$K_d = \frac{d^2(1-\sigma)^3}{36\sigma^2 H_k}$$ Eq. [2.3.7]

$$\frac{1}{K} = \frac{1}{K_{fiber}} + \frac{1}{K_d}$$ Eq. [2.3.8]

Another study on mathematical modeling of RTM process is conducted by Erdal and her colleagues [43]. Darcy Law equation is used for modeling incompressible flow. Additionally, in order to define mass conservation, its' assumed that particle diameter is under 1μm so no diffusion phenomena. Then mass balance equation is determined as in equation 9.

$$\frac{\partial[\varepsilon C]}{\partial t} + (\varepsilon v)\nabla C + \frac{\partial \sigma}{\partial t} = 0$$ Eq. [2.3.9]

Re-suspended retained particles (σ_u) are taken into consideration in filtration kinetics and equation 10 is used to make calculation of filtration. In that equation α is filtration coefficient and an empirical constant like σ_u, V' is Darcy velocity.

$$\frac{\partial \sigma}{\partial t} = \alpha UC - \sigma_u \sigma$$ Eq. [2.3.10]

In this paper filtration coefficient calculation model is also written in terms of specific surface area (Eq. 2.3.11). Where S is the specific surface area of preform and S_0 is the total specific surface area of preform and deposited particles.

$$a = a_o \frac{S}{S_0}$$

Eq. [2.3.11]

Kozeny-Carman relation is used for the basis of permeability definition. The grain model is accepted which assumes that deposition of the particles is uniformly distributed around fibers and does not contact each other and flow passage gets narrow. The basis on these and relation between permeability, porosity and filtration coefficient, local permeability equation becomes a function of porosity an initial permeability as Eq. 2.3.12 in which α_2 is an empirical constant.

$$K = K_0 \left[\left(\frac{\varepsilon}{\varepsilon_0} \right) \left(\frac{1 - \varepsilon}{1 - \varepsilon_0} \right)^{-4} \right]^{a_2}$$

Eq. [2.3.12]

Resin fluid is assumed to be a Newtonian fluid. Therefore, its' shear stress thinning dependence is small. A viscosity definition with constant shear rate change is used in this study (Eq. 2.3.13). As presented at Eq. 2.3.13. μ_0 is initial viscosity value, C is instant concentration value of filler particle and A is an empirical value (actually its' defined as max. particle volume concentration of filler particles [57].

$$\mu = \mu_0 \left(1 - \frac{C}{A} \right)^2$$

Eq. [2.3.13]

Additional mathematical model for RTM and VARTM processes under constant injection pressure applied to dual scale fibrous medium constructed by Zhou and colleagues [58]. Average flow velocity is calculated via Darcy Law and for mass flow estimation, control volume technique is used which is implicated as Eq. 2.3.14 mathematically. In this formula time derivation of saturation (s) instead of retention rate.

$$A.u = Adx.v_t \emptyset_{tf} \frac{\partial s}{\partial t} + A\left(u + \frac{\partial u}{\partial x}.dx\right)$$ Eq. [2.3.14]

In equation 14 v_f is the tow volume fraction and $\emptyset_{tf}$ is the porosity in the tow. Saturation rate in the Eq.14 is dependent on a constant (c) and pressure (P).

$$\frac{\partial s}{\partial t} = cP$$ Eq. [2.3.15]

And permeability is defined in terms of viscosity, flow velocity, and preform porosity ($\emptyset_f$) (Eq. 2.3.16).

$$K = \mu\left(\frac{Q}{A}\right)^2 / (\frac{\partial p}{\partial t}\emptyset_f)$$ Eq. [2.3.16]

Chapter 3

3 Adopted Mathematical Model

A mathematıcal model for this study is adopted from Erdal et al. [43], Lefevre et al. [44,55] and Herzig [59].

3.1 Flow Model

In this study, resin flow is going to be analyzed at the macro-level, and the fluid resin is a Newtonian and isotropic fluid.

General definition of an incompressible flow through porous media is done by Darcy equation. Darcy Law in 1-D may be written as in Eq. 3.1. Darcy equation is commonly used to evaluate the porous medium flow parameters such as: permeability, flow velocity, permeability and pressure gradient [27,31,32,38,43,44,54,58,60–64].

$$U = \varepsilon * V = -\frac{K}{\mu}\Delta P \qquad\qquad \text{Eq. [3.1]}$$

In the Darcy equation, Darcy velocity is defined with U and V is front flow velocity. ε is total porosity of the medium, μ is viscosity of the resin, K is permeability of the preform and ΔP is pressure difference .

Darcy Law gives a linear relationship between velocity and pressure drop, and it is very consistent at very low Reynolds number [54,62,65], and it works perfectly where Re number is close to 1 [54,66]. Also, Darcy Law is valid for $0 \leq Re \leq 4$ [67] and $0 \leq Re \leq 10$ [68]. However, Darcy formulation does not include inertial

force term, and inertial forces become dominant, thus pressure drop-velocity relationship turn into quadratic function at high Reynolds Numbers, which are bigger than critical Reynolds Number [69], and correctness of Darcy Law becomes doubtful over as the Reynolds number increases [70]. In this study high viscosity resin flow through the highly porous media at the order of 10^{-15}, thus at macroscopic level the, flow is expected to be a creeping flow with very low Reynolds Numbers. In Darcy regime inertial forces and kinetic energy are negligible when viscous forces are taken into consideration [71]. Therefore, inertial forces are neglected and, any extensions for inertial forces like Forcheimmer's formula is not taken into consideration.

Porosity (ε) depends on the initial preform porosity value (ε_0), deposited particle rate (retention-σ) and entrapped liquid rate (β) between the deposited particles. Initial porosity is the free area through the bulk preform and evaluated via takin into consideration volume of fibers and bulk preform. Initial porosity is expressed by Eq. 3.2. It is evaluated as in equation 3.3.

$$\varepsilon_0 = 1 - \frac{Volume\ of\ Fibers}{Volume\ of\ Bulk\ Reinforcement} \qquad \text{Eq. [3.2]}$$

$$\varepsilon = \varepsilon_0 - \beta\sigma \qquad \text{Eq. [3.3]}$$

This definition of porosity shows that porosity tends to decrease with time due to clogged particles. Also, entrapped liquid presence change with time depending on initial β value (β_0), an empirical constant r and retention rate as shown in Eq. 3.3. Empirical constant r will be determined later via experiments but until that it is taken 30 according to Lefevre et. al. study [44].

$$\beta = \beta_0 - r\sigma \qquad \text{Eq. [3.3]}$$

3.2 Filtration Model

During resin flow mass conservation must be satisfied, so a mass conservation expression must be defined. While defining this equation retention factor must be taken into consideration. Mass conservation equation can be defined as in Eq. 3.4.

$$\varepsilon \frac{\partial C}{\partial t} + U \frac{\partial C}{\partial x} = (\beta_0 C - 2rC\sigma - 1)\frac{\partial \sigma}{\partial t} \qquad \text{Eq. [3.4]}$$

In mass balance definition an additional function takes role which is derivative of retention respect to time which depends on filtration coefficient (Eq. 3.5)

$$\frac{\partial \sigma}{\partial t} = kF(\sigma)UC - k_r\sigma \qquad \text{Eq. [3.5]}$$

Factors of this expression is filtration coefficient (k), Darcy velocity (U), concentration (C), retention rate (σ), retention function ($F(\sigma)$) and possibility of retained particle re-suspension (k_r) [59]. An initial filtration coefficient k_0 is determined depending on the preform structure and material. Re-suspended retained particle rate is ignored due to constant pressure injection and flow direction [55]. Then final derivation of retention respect to time derives to Eq. 3.6.

$$\frac{\partial \sigma}{\partial t} = kF(\sigma)UC \qquad \text{Eq. [3.6]}$$

Also, retention function may be defined by an approach as equation 3.7 [72].

$$F(\sigma) = 1 - k\sigma \qquad \text{Eq. [3.7]}$$

The relation between initial filtration coefficient and filtration coefficient is taken equal to proportion of instant porosity and initial porosity as in Eq. 3.8 [59].

$$\frac{k}{k_0} = \frac{\varepsilon}{\varepsilon_0}$$

Eq. [3.8]

3.3 Viscosity

In this study fluid resin is a Newtonian fluid. Under the assumption of constant shear rate effect on viscosity is expressed as in Eq. 3.9 [43,57].

$$\mu = \mu_0 \left(1 - \frac{C}{A}\right)^{-2}$$

Eq. [3.9]

C is the volume fraction of the particles in the resin, μ_0 is the viscosity of the pure resin and A is a constant. A constant is equal to 0.680 due to smooth sphere shape of particles [57].

3.4 Permeability

In our system has two distinct permeability values which are fiber and deposited particle permeability. These two values are taught as parallel system values, and this system evolves in time due to deposited particle profile. Calculation of the total permeability is performed by equation 3.10 [44].

$$\frac{1}{K} = \frac{1}{K_{fiber}} + \frac{1}{K_d}$$

Eq. [3.10]

K_{fiber} is a constant value of empty preform depending on the fiber volume fraction. However, evaluating deposited particle permeability is a more complicated

phenomenon. Kozeny-Carman relationship may be used to evaluate the permeability [44,61,64,73]. Kozeny-Carman permeability relationship is used to evaluate deposited particle permeability, and it depends on retention rate (σ), Kozeny constants (H_k) and particle diameter (d) Eq. 3.11 [44].

$$K_d = \frac{d^2(1 - \sigma)^3}{36\sigma^2 H_k} \qquad \text{Eq. [3.11]}$$

Kozeny constant is defined as $36H_k$ is equal to 150 from Ergun's experimental results for granular media [44,74].

Chapter 4

4 Simulation Tools

4.1 Flow Front Tracking

In fluid flow, numeric analysis flow front is needed to be determined precisely. Flow front is an essential subject to determine fluid motion phenomena in terms of computation of variables and stability of motion, so we needed a method able to track moving interfaces. There are several flow front tracking methods, and some of them are Volume of Fluid (VOF), Phase Field and Level Set methods.

4.1.1 Volume of Fluid Method (VOF)

The volume of the Fluid method is developed by Hirt and Nichols. VOF is based on fractional volumes of fluid which are called control volume and generally used modeling motion of two or more fluids which are immiscible. In that method, fluid/fluid interfaces and solid boundaries are the subjects to be considered [75]. VOF fluid method tracks the free interface between two fluids so all control volumes must include one of the fluids. If one fluid in question a compressible ideal gas can be defined as second fluid [76]. VOF method works very well with 1-D problems. However, reconstruction of the interface in each cell becomes difficult to calculate at two or more dimension problems [77].

Unfortunately, in two-phase VOF bubbles can be formed because VOF tries to satisfy a very low contact angle condition [78]. Also, all phases move independently through each other rather than one phase moving into another phase.

4.1.2 Phase Field Method

Diffusing interface logic bases the Phase Field method which was considered by van der Walls firstly in late 19th century and Phase field equations were developed by Chan and Hilliard [79].

Phase Field method aims to track the interface between two immiscible fluids. The motion of this interface is determined by minimizing free energy of a system that is why Phase Field calculates two more transportation equation (Chan-Hilliard equation and continuity equation) besides modified Naiver-Stokes equations to be sure that advection does not change total energy of the system.

Due to Phase Field method has more variables to be determined and Chan-Hilliard equation can rise to the 4th-degree partial differential equation which needs more difficult calculation sequence than Level Set Method [80]. Also, precise definition of phase characterization and providing high grid number near interface are essential to get correct movement of interface [81].

4.1.3 Level Set Method

The level Set method was emerged as an idea of Osher and Sethian in 1987 [82]. The level Set method is similar to VOF and Phase Field methods but it based two domains separated with one interface simulations. This method works with an explicitly segregated inside and outside regions of interface [83]. A mathematical formulation is used to advance flow in a normal direction at a certain speed and changes interface topology [81]. As an advantage Level Set model has relatively simple and easy to solve due to its' smooth formulation which lessens computational work and memory need.

However, the volume of fluid may not always be preserved during advection of interface, and it may be needed to be corrected [77].

Level Set Method was preferred because of its' easiness to imply. COMSOL©️ Multiphysics includes Level Set method as a built-in function module.

4.2 Porous Media Flow

As mentioned in section 3, in that model Darcy Law will be used as momentum transfer equation to propagate fluid. Also, Darcy Law includes porous media flow characteristics like porosity and permeability of both media and fluid. Darcy Law is defined as a module in COMSOL[©].

4.3 Mass Conservation and Filtration Kinetics

In Section 3.2 mass conservation and filtration equations were explained.

4.3.1 Mass Conservation Equation

Mass conservation was defined regarding concentration (C) in Eq. 4.1.

$$\varepsilon \frac{\partial C}{\partial t} + U \frac{\partial C}{\partial x} = (\beta_0 C - 2rC\sigma - 1) \frac{\partial \sigma}{\partial t} \qquad \text{Eq. [4.1]}$$

As seen above it is needed some built-in mathematical functions to be used in defining mass conservation and filtration physics. In COMSOL[©] under mathematics module, partial differential equation definitions are present and can be used to define mass conservation and filtration kinetics by arranging coefficients in the formulations.

Mass conservation can be defined with a coefficient form of PDE module in COMSOL[©] (Eq. 4.2).

$$e_a \frac{\partial u}{\partial t^2} + d_a \frac{\partial u}{\partial t} + \nabla(-c\nabla u - \alpha u + \gamma) + \beta * \nabla u + au = f \qquad \text{Eq. [4.2]}$$

Variable u is defined as concentration (C). Other parameters are e_a, d_a, c, α, ɣ, β, a and f to be determined as; $e_a = 0$, $d_a = dl.\,epsilon$, $c = 0$, α = 0, ɣ = 0, a =

0, $\beta = dl.u$, $\beta = dl.v$. By substituting these values Eq. 4.2 becomes as in Eq 4.3.

$$f = (\beta_0 C - 2r\sigma C - 1)\frac{\partial \sigma}{\partial t}$$ Eq. [4.3]

Then equation 3.4 is obtained as an input module.

4.3.2 Filtration Equation

Filtration physic equation was explained as in Eq. 4.4.

$$\frac{\partial \sigma}{\partial t} = kF(\sigma)UC$$ Eq. [4.4]

An assumption of $F(\sigma)=0$, can be done due to lack of experimental data of $F(\sigma)$ [44] and its' ignorable effect on retention .

In order to define filtration equation, COMSOL[©]'s general form of PDE built-in mathematical model can be used (Eq. 4.5).

$$e_a \frac{\partial^2 u}{\partial t^2} + d_a \frac{\partial u}{\partial t} + \nabla\Gamma = f$$ Eq. [4.5]

This built-in mathematical module evolves to our filtration model by defining variable u as retention (σ) and $e_a = 0$, $d_a = 1$, and $\Gamma = 0$.

By substituting these values in Eq. 4.5, Eq. 4.6 is obtained.

$$f = k * F(\sigma) * |dl.u| * C$$ Eq. [4.6]

Chapter 5

5 Results & Discussion

5.1 Flow Front Tracking

As mentioned in Chapter 4 Level Set method is used for estimation of the flow front position during the filling process. The position of the flow front is analyzed via Level Set Method and calculated analytically to ensure that they are compatible each other.

Darcy Law [Eq. 3.1] is the constitutive equation which gives the relationship between pressure gradient and velocity, thus it is used to calculate the flow front position calculation analytically. 1-D Darcy Law is derived to Eq. 5.2 to get position directly as showed below.

$$U = \varepsilon * v = -\frac{K}{\mu}\Delta P = Q/A$$ Eq. [5.1]

$$x = \frac{UAt}{A\varepsilon_o}$$ Eq. [5.2]

5.1.1 Simulation 1: Homogeneous Media Constant Velocity Side Filling Model

Firstly, Level Set's capability of following flow front should be examined so analytical and numeric solutions are compared if they are coherent or not. Our preform thickness is 1mm and length is 10 mm. From the analytical calculation, t_{fill} is expected to be about 8.3s. In order to understand if COMSOL$^{©}$ Level Set

module meets with the analytical value, a simplified model is constructed. This model consists of just Level Set and Darcy's Law modules and does not include mass conservation and retention effects. At the end, it is seen that this model's numerical results and analytical solution of Darcy's Law are pretty close each other. Figure 14 indicates inlet and outlet gates of the preform.
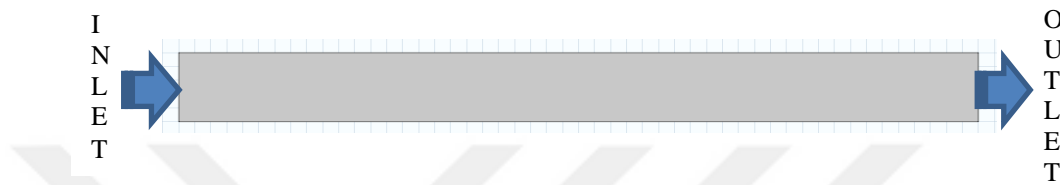
Figure 5.1 Inlet and Outlet Gates of Simulation 1

All the parameters of Darcy, geometry and Level Set Methods were defined as input are given in Table 5.1.

Table 5.1 COMSOL Parameters of Simulation 1

Geometry	
Width	10 mm
Height	1 mm
Darcy Parameters	
Inlet Velocity	0.001 m/s
Outlet Pressure	0 Pa
Density (ρ)	1100 Kg/m^3
Permeability (K)	1e-12 m^2
Porosity (ε)	0.813
Viscosity (μ)	0.01 Pa*s

Level Set Parameters	
Reinitialization Parameter (γ)	0.0005
ε_{ls}	ls.hmax/2

Flow front position comparison of analytical and numerical solutions are showed in Figure 5.2. Line graph represents the analytical results, and the points represent the numeric results.

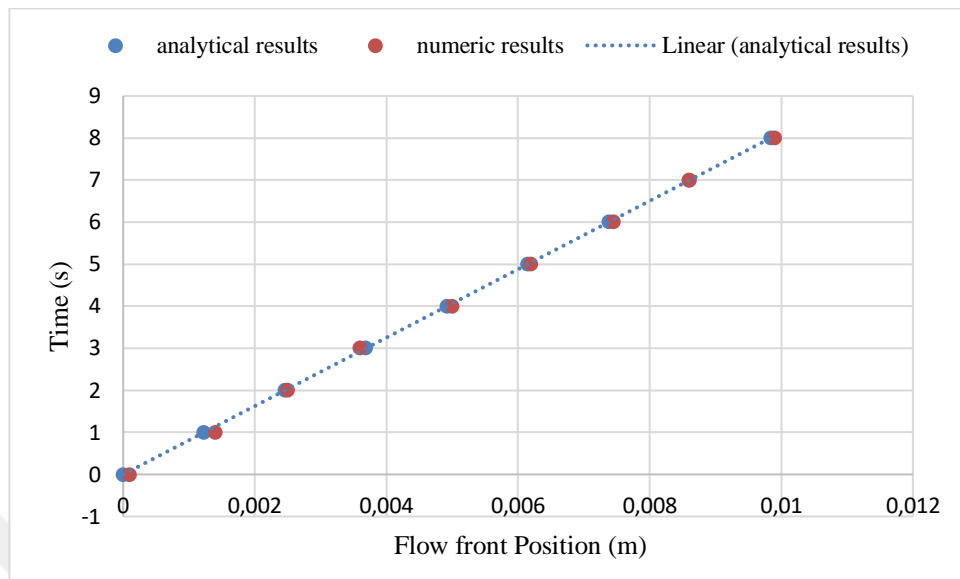**Figure 5.2 Flow Front Result Comparison of Analytical and Numeric Solutions**

5.2 Side Filling Models

5.2.1 Simulation 2: Heterogeneous Media Constant Pressure Side Filling Model

In this study, RTM production process for layer by layer heterogeneous preform production with two different permeability value was analyzed. Therefore, firstly a dual permeability COMSOL$^{©}$ model with simplified double layer geometry was conducted to observe the RTM characteristics of this type of preform. Again filtration phenomenon is ignored, and only Darcy's Law and Level Set modules were used and filling characteristics of the parts were compared considering two different materials with 1E-12 and 1E-15 m^2 permeability values. At the top 0.2 mm, thick low permeability material was defined and belove of that high

permeable   material   placed   which   can   be   seen   in   Figure   16.
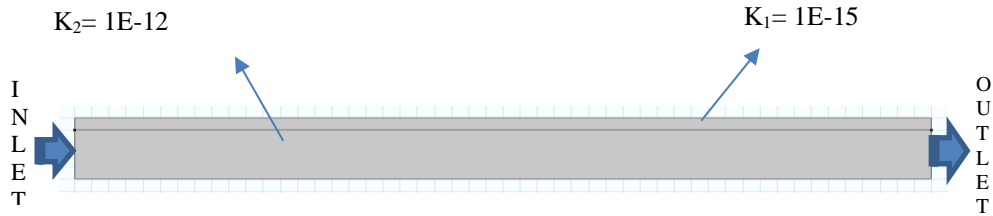

Figure 5.3 Dual Permeability Preform Simplified Geometry for Simulation 2

This model constructed over constant pressure difference and parameters in Table 5.2 were determined and used as input in order to be compatible with our fabrication equipment which will be performed in the future.

Table 5.2 COMSOL Parameters of Simulation 2

Geometry	
Width	10 mm
Height	1 mm

Darcy Parameters	
Inlet Velocity	
Outlet Pressure	1e5 Pa
Density (ρ)	0 Pa
Permeability (K)	1100 Kg/m^3
Porosity (ε)	1e-12*(y<0.0008)+1e-15*(y>=0.0008) m^2
Viscosity (μ)	0.813

Level Set Parameters	
Reinitialization Parameter (γ)	0.00025
ε_{ls}	ls.hmax/2

Flow front position results are shown in Figure 5.4. Red color represents the filled areas, and blue color represents the empty areas of the preform.
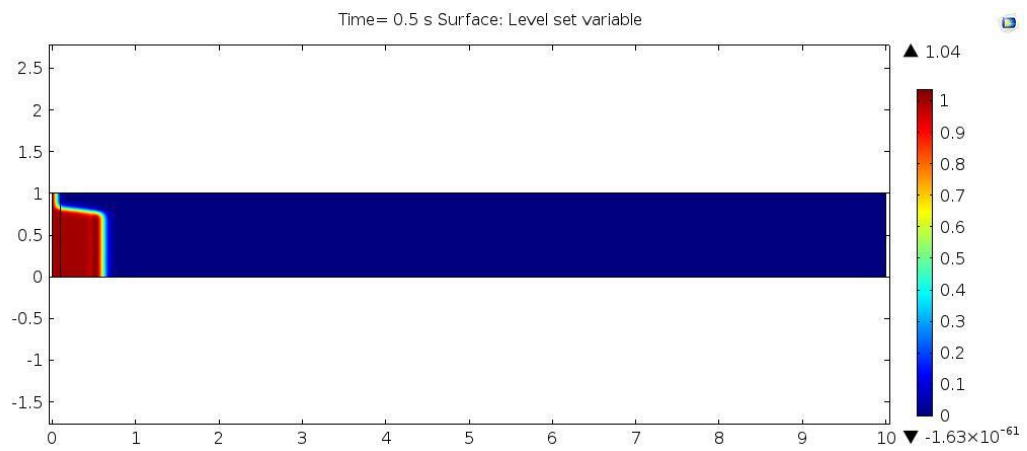
(a)
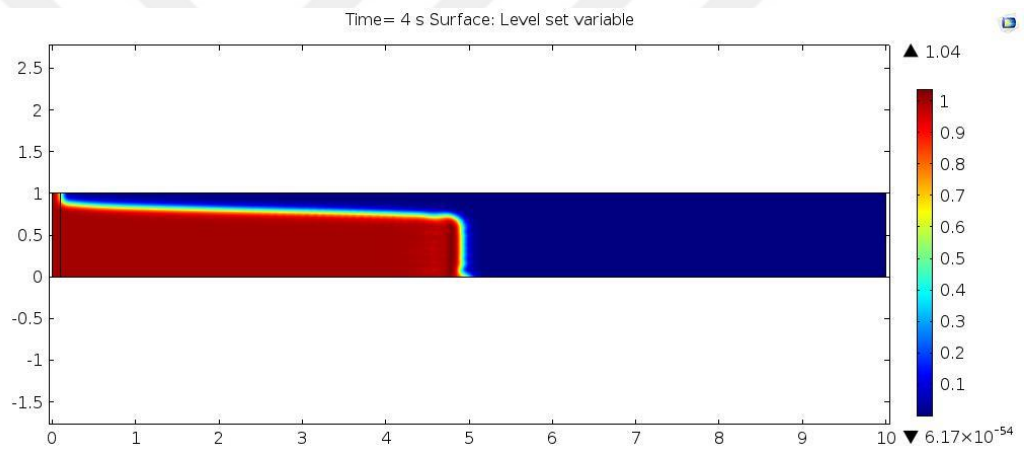
(b)

(c)

Figure 5.4 Dual Permeability Flow Front Analyze Results Under Constant Pressure t=0.5s (a), t=4s (b), t=8.2s (c)

As seen in Figure 5.4 flow front line showed an uneven advancement during the RTM process due to permeability difference. At the end of the process, there would be a big void in the preform which is an unwanted situation.

5.2.2 Simulation 3: Heterogeneous Media Staggered Layers with Constant Pressure Side Filling Model
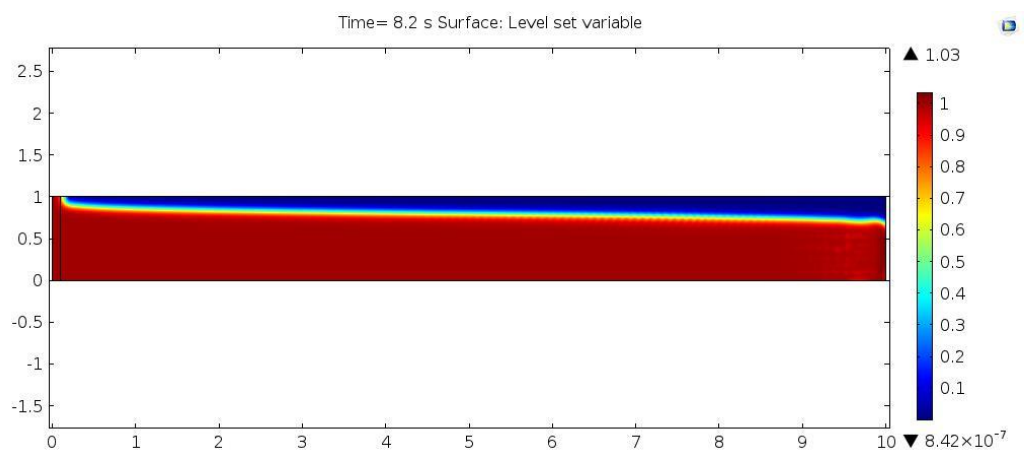
Another analysis was conducted with the geometry of composite material, which is planned to be fabricated later, to see what would be the flow characteristic with side boundary injection logic. As indicated in Figure 5.5, simulation geometry has 6 mm thickness with six 1 mm thick packages of dual scale materials and 10 mm length.
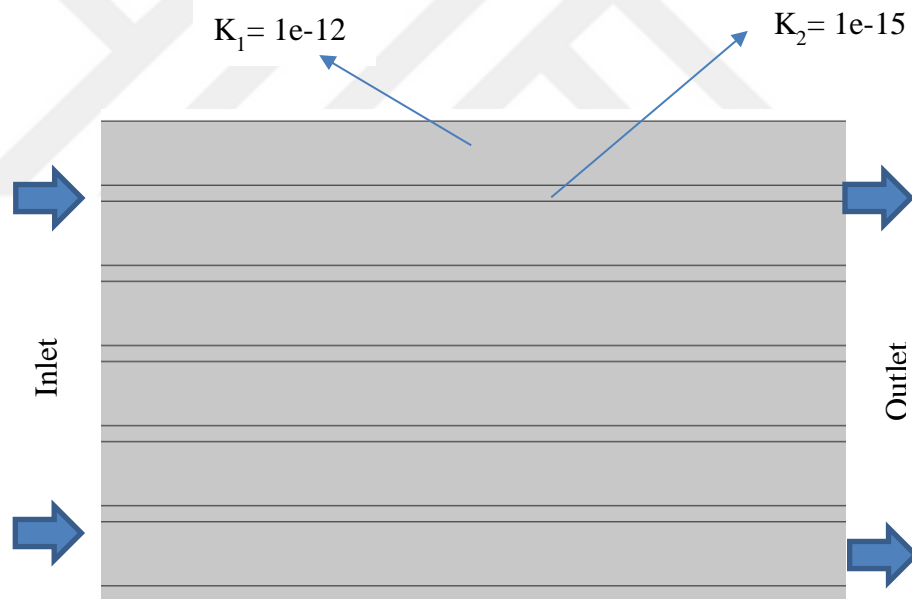

Figure 5.5 Staggered Heterogeneous Media Geometry for Simulation 3

Additionally, constant pressure boundary conditions were applied, and filtration was ignored and related parameters are shown in Table 5.3.

Table 5.3 COMSOL Parameters for Simulation 3

Geometry

Width 1	1 mm
Height 1	0.2 mm
Width 2	1 mm
Height 2	0.8 mm

Darcy Parameters

Inlet Pressure	1e5 Pa
Outlet Pressure	0 Pa
Viscosity (ρ)	1100 Kg/m^3
Permeability (K_1)	1e^{-12} m^2
Permeability (K_2)	1e^{-15} m^2
Porosity (ε)	0.813
Dynamic Viscosity (μ)	0.01 Pa*s

Level Set Parameters

Reinitialization Parameter (γ)	0.0005
ε_{ls}	ls.hmax/2

From this model again immiscible flow paths creating big voids are expected between all individual layers. Results of this simulation at various process times are shown in Figure 5.5, and void formation can be seen for various time steps.

(a)

Time= 4 s Surface: Level set variable

(b)

Time= 8.1 s Surface: Level set variable
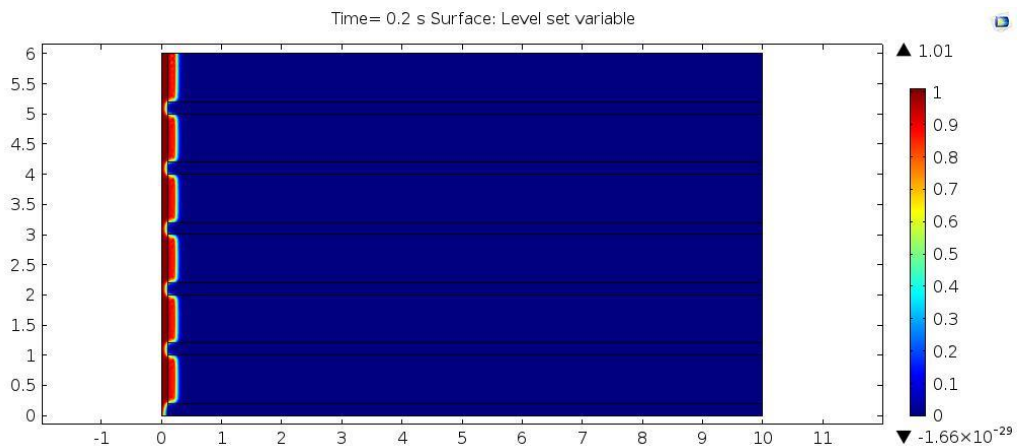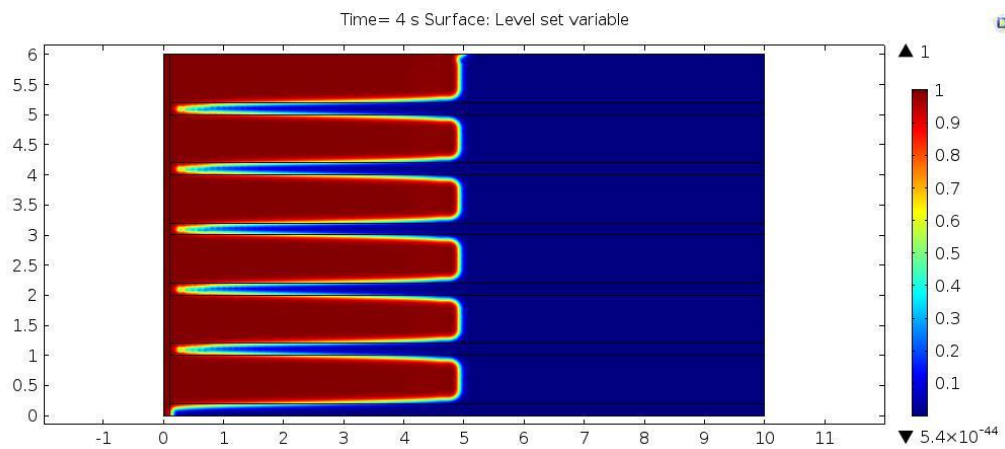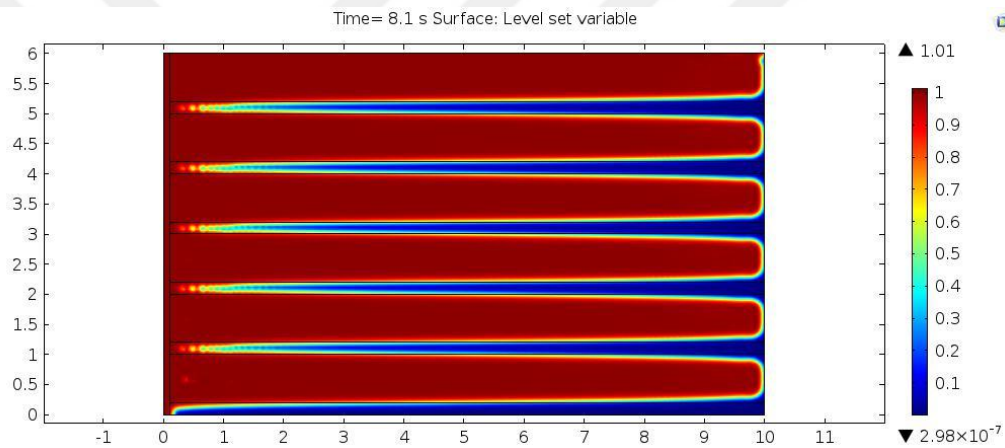
(c)

Figure 5.6 Flow Front Tracking Results of Heterogeneous Staggered Layer Preform Under Constant Pressure t=0.2 (a), t=4 (b), t=8.1 (c)

In the results fingering flows can be observed. These viscous fingering flows are evolved due to the heterogeneity of permeability which effects fluids advancement capability. As a result of permeability difference, fluid flow through less viscous (in high permeable part) material easier than the higher one. Therefore, one flow front moves relatively faster and streamline will be unstable [84,85].

It is understood that traditional RTM method is not capable of filling this type of preform from side boundaries. Thus an alternate filling process should be taken into consideration.

Therefore, determining the position of resin injection becomes an essential issue due to the presence of void formation. As an alternate method, CRTM process logic can be taken into consideration to obtain a uniform filled product and inlet gate moved to the top boundary of the preform.

5.3 Heterogeneous Media Top Filling Models

5.3.1 Simulation 4: Simplified Geometry Heterogeneous Media Model with Constant Velocity

A simulation with simplified heterogeneous preform geometry consisting of one layer of each permeability conducted to understand how CRTM logic works when applied to RTM production method.

In that model geometry defined with low permeability material with 0.2 mm thickness at the top and remaining part is represented high permeability material. This simplified geometry with heterogeneous media was used to compare analytical and numerical advancing results. The geometry of preform is similar to side filling one, but inlet gate is positioned at the top as seen in Figure 5.7.
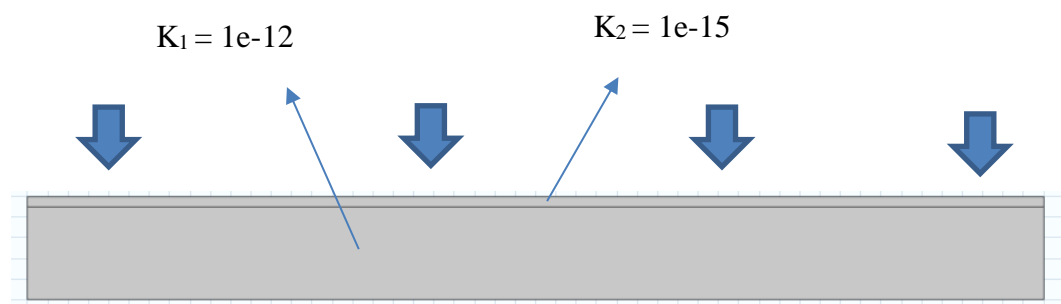
Figure 5.7 Simplified Top Filling Simulation Geometry

In that model, CRTM logic was applied to RTM production method. Simulation parameters are presented in Table 5.4.

Table 5.4 COMSOL Parameters for Simulation 4

Geometry	
Width	10 mm
Height	1 mm
Darcy Parameters	
Inlet Velocity	0.001 m/s
Outlet Pressure	0 Pa
Density (ρ)	1100 Kg/m^3
Permeability (K)	1e-15*(y<0.0002)+1e-12*(y>=0.0002) m^2
Porosity (ε)	0.813
Viscosity (μ)	0.01 Pa*s
Level Set Parameters	
Reinitialization Parameter (γ)	0.0003
ε_{ls}	ls.hmax/3

Results of CRTM logic simulation results are indicated in Graph 2, and as it can be seen that analytical and numeric solutions are coherent each other in terms of filling time, so it is convenient to fill the resin from a top positioned gate.

Figure 5.8 Comparison of Numeric and Analytical Solutions of Top Filling Method

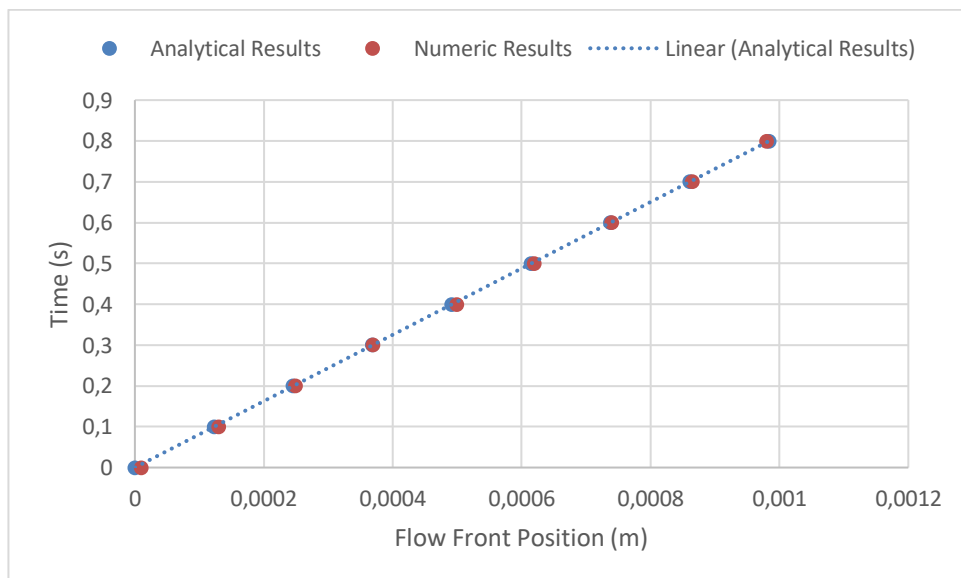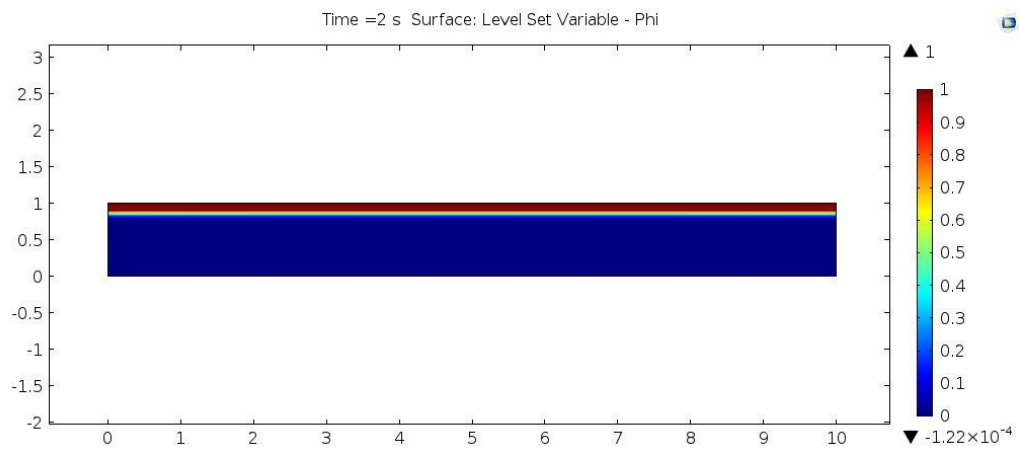### 5.3.2 Simulation 5:Heterogeneous Simplified Geometry Media Model with Constant Pressure Top Filling

Inlet boundary conditions of simulation 3 was changed to under constant pressure. The geometry of simulation preform is same with simulation 3 and input parameters are shown in Table 5.5.

Table 5.5 COMSOL Parameters for Simulation 5

Geometry	
Width 1	1 mm
Height 1	0.2 mm
Width 2	1 mm
Height 2	0.8 mm
Darcy Parameters	
Inlet Pressure	1e5 Pa
Outlet Pressure	0 Pa
Density (ρ)	1100 Kg/m^3
Permeability (K)	1e-15*(y<0.0002)+1e-12*(y>=0.0002) m^2
Porosity (ε)	0.813
Viscosity (μ)	0.01 Pa*s
Level Set Parameters	
Reinitialization Parameter (χ)	0.00005
ε_{ls}	ls.hmax/2

The filling gate is moved from the left boundary to the top boundary so RTM process would be performed via CRTM logic in order to avoid permeability difference and flow direction interaction leaded void formation. This time fluid would pass through materials one by one as layers at a time so, it was expected to obtain much more homogeneous average front flow velocity which means fewer voids in the filled part as shown in Figure 5.9.

(a)
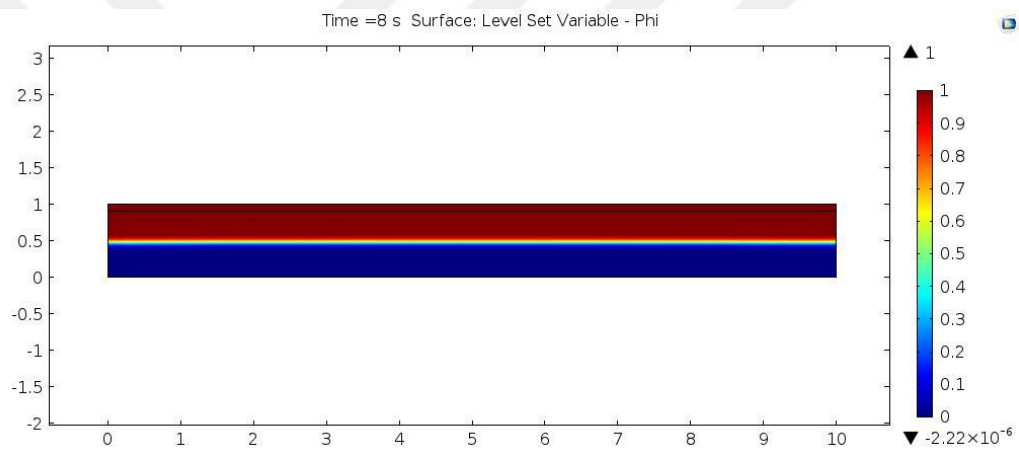
(b)
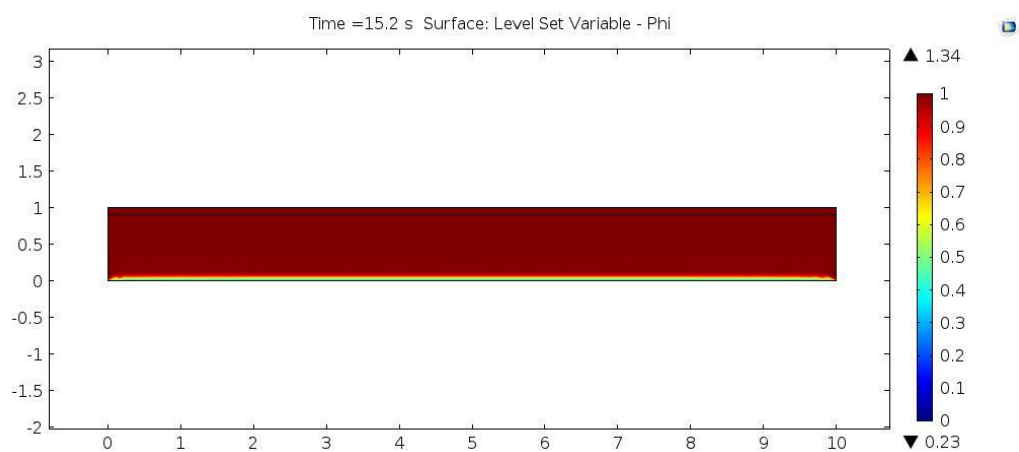
(c)

Figure 5.9 Top Filling Simulation Under Constant Pressure Results of Dual Permeability Simplified Preform t=2s (a), t=8s (b), t=15.2s (c)

5.3.3 Simulation 6: Heterogeneous Media Staggered 6-Layer Model with Constant Pressure Top Filling

As simulation 4 demonstrates via top filling method, a homogeneous filled material can be produced. Therefore, this method can also be used for 6 group of layer geometry. An additional model was constructed with 6 layers of dual permeable structure as simulation 3 geometry with no filtration effect with constant pressure injection from the top boundary (Figure 5.10).

Figure 5.10 Geometry of Heterogeneous Staggered Layers Geometry for Simulation 6
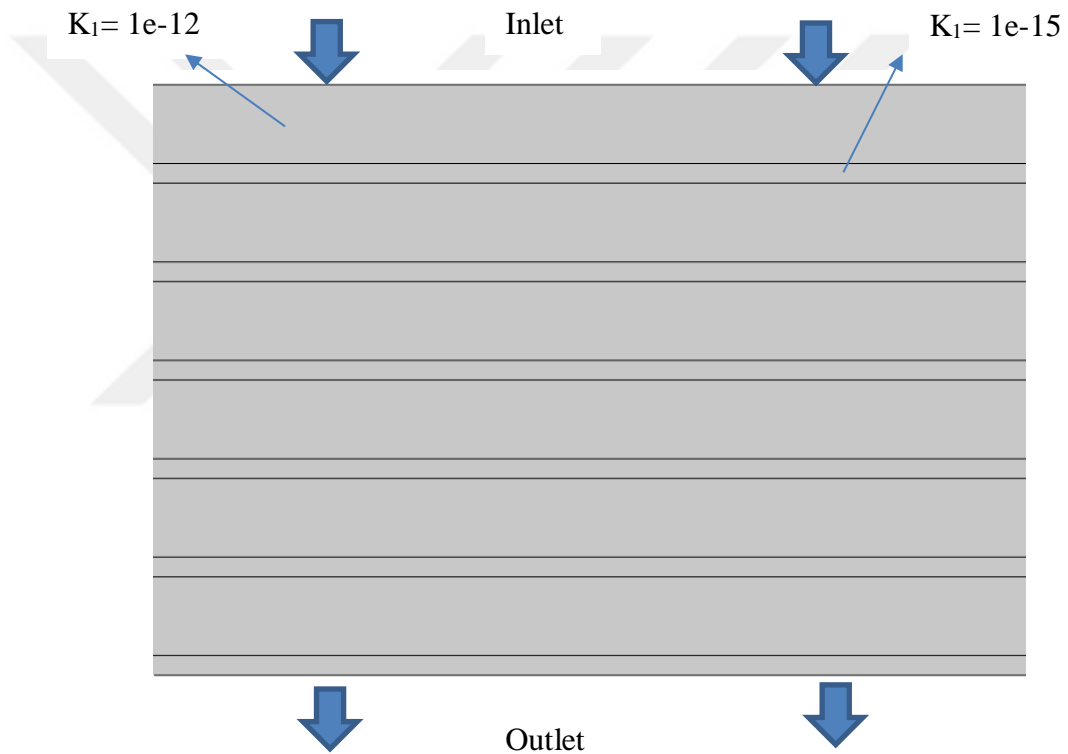
Simulation parameters were inputted as in Table 5.6.

Table 5.6 COMSOL Parameters for Simulation 6

Geometry	
Width 1	10 mm
Height 1	0.2 mm
Width 2	10 mm
Height 2	0.8 mm

Darcy Parameters	
Inlet Pressure	$1e^5$ Pa
Outlet Pressure	0 Pa
Density (ρ)	1100 Kg/m^3
Permeability (K) 1	$1e^{-12}$ m^2
Permeability (K) 2	$1e^{-15}$ m^2
Porosity (ε)	0.813
Viscosity (μ)	0.01 Pa*s

Level Set Parameters	
Reinitialization Parameter (γ)	3 e-5
$\boldsymbol{\varepsilon_{ls}}$	ls.hmax/3

Figure 5.10 demonstrates that staggered position of one each group of low and high permeable materials can be filled precisely via filling from the top. However, a small acceptable finger flow effect occurs as the fluid resin passes through each permeability boundaries. This effect gets bigger as the flow advances through more permeability transition borders. Fortunately, 6-layer geometry does not evolve in poor flow characteristics as seen in Figure 5.11.

(a)

Surface: Time= 290 s Level set variable phi

(b)

Surface: Time= 584 s Level set variable phi
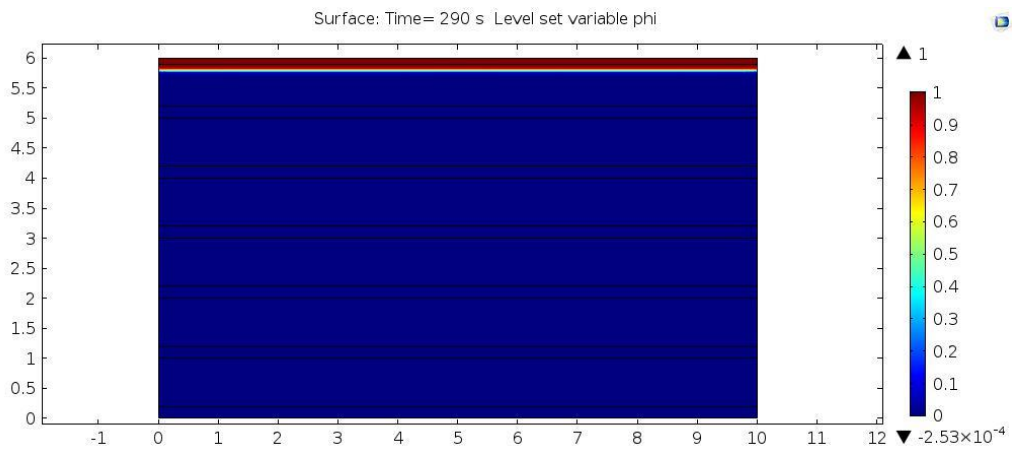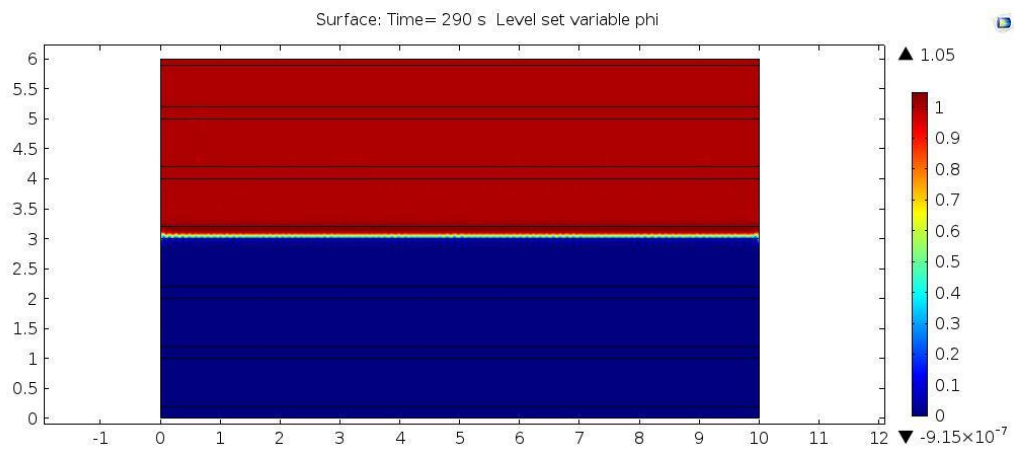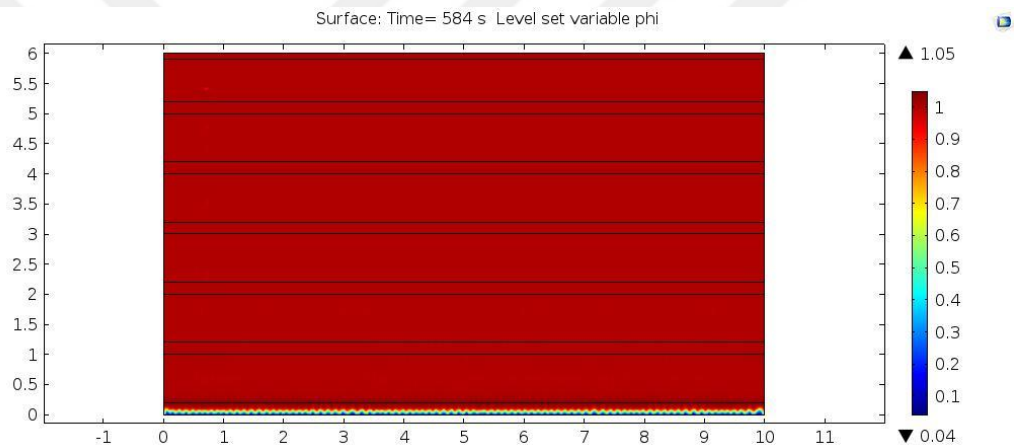
(c)

Figure 5.11 Up Filling Laminate Preform Under Constant Pressure Model Flow Front Tracking Results t=20s (a), t=290s (b), t=584s (c)

5.3.4 Simulation 7: Simplified Heterogeneous Media Model with Constant Pressure Top Filling and Filtration

As next step, filtration model is introduced to the simplified heterogeneous media model. In that model concentration (C), dependent viscosity and porosity definitions are defined. Also, fiber's effect on permeability, definition, filtration (β) and retention (σ) factor equations are introduced to that model. Concentration equation provides homogeneity profile which is desired to be equal to initial concentration value. Filtration coefficient (β), and retention (σ) value are expected

to reach their maximum value near to the inlet gate. This model's initial parameters are defined in Table 5.7.

Table 5.7 COMSOL Parameters for Simulation 7

Geometry	
Width 1	1 mm
Height 1	0.2 mm
Width 2	1 mm
Height 2	0.8 mm

Darcy Parameters	
Inlet Pressure	1e5 Pa
Outlet Pressure	0 Pa
Density (ρ)	1100 Kg/m^3
Permeability (K)	1/(1/(5e-15*(y>=0.2)+1.5e-17*(y<0.2))+(36*Hk/(d^2*(1-sigma)^3)))
d	0.012 mm
H_k	4.167
Initial Porosity (ε_0)	0.813
Viscosity (μ_0)	0,3 Pa*s
A	0.68

Level Set Parameters	
Reinitialization Parameter (γ)	0.00005
ε_{ls}	ls.hmax/2.5

Filtration Parameters	
Initial beta (β_0)	5,15
r	30
Initial Filtration Coefficient (k_0)	0.0157
Initial Concentration (C_0)	0.30

Front flow track results are shown in Figure 5.12 and as seen in the Figure, filtration effect dramatically decreases the flow velocity in the porous media. Results for 5 different time were given. When time steps are compared it can be interpreted that filtration effect during flow makes flow speed slow down because filling time gets longer as resin advances in porous media while filtered particles clog the flow path.

So, in Figure 5.12, filtration effect is obvious that in 300-minute resin passes 1/3 of the preform, but between 700 and 1000 minutes it could not advance as fast as it did at the beginning. Also, this clogging effect can be found out from Figure 26a in which maximum particle concentration reaches to nearly 2 mm thickness after 300 m time. Also, after 1465 minutes (Figure 5.12 c) when the front flow reaches to the 1 mm thickness, not half of the preform is particle filled with maximum concentration, so more filling time is needed to get maximum particle deposition in the whole preform.
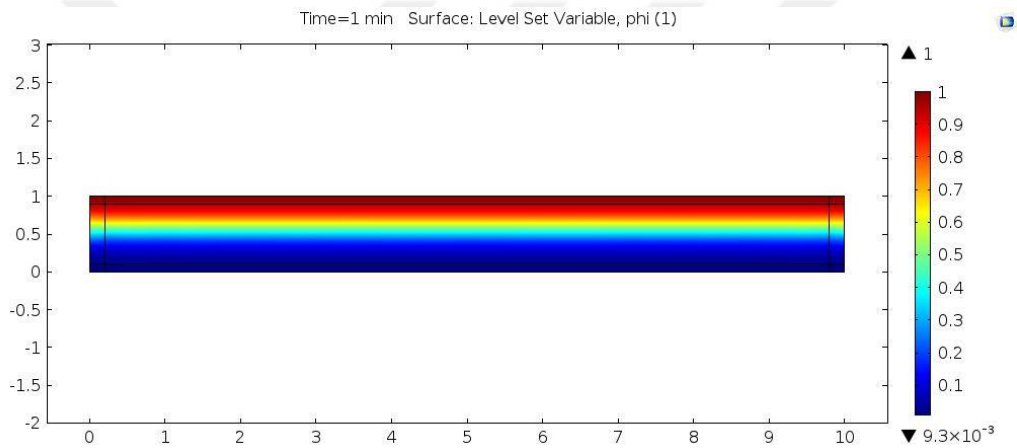
(a)
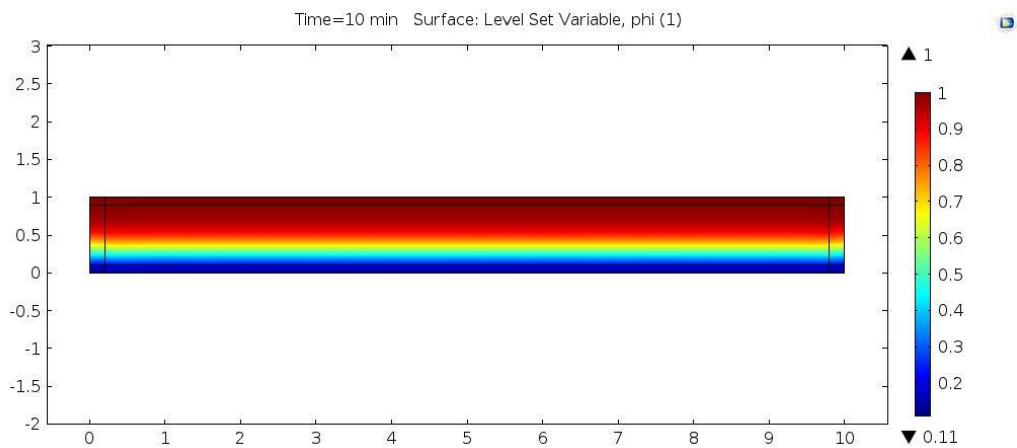
(b)
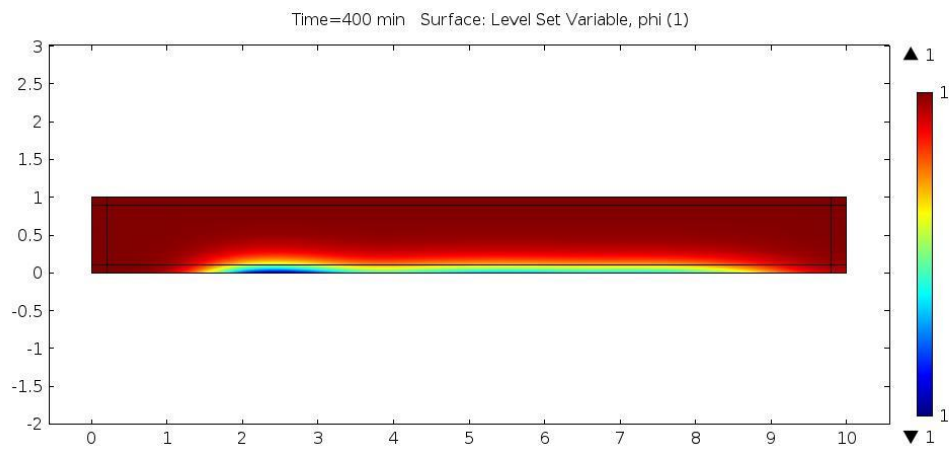
(c)
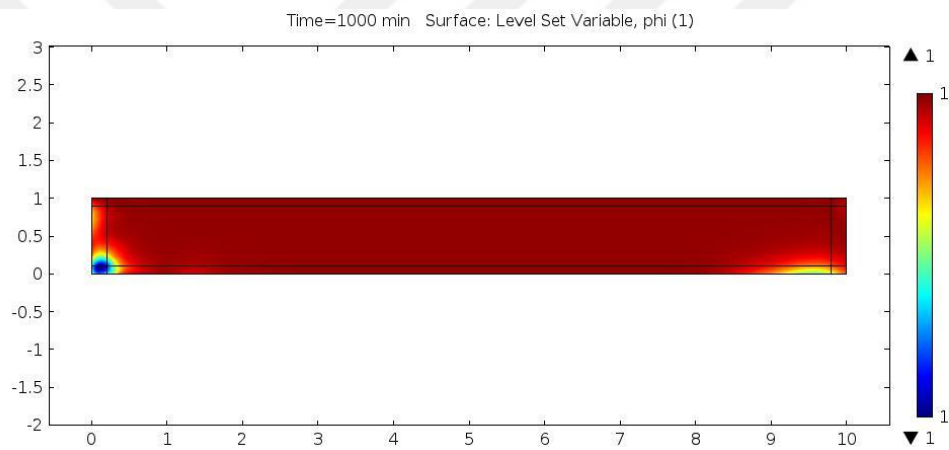
(d)
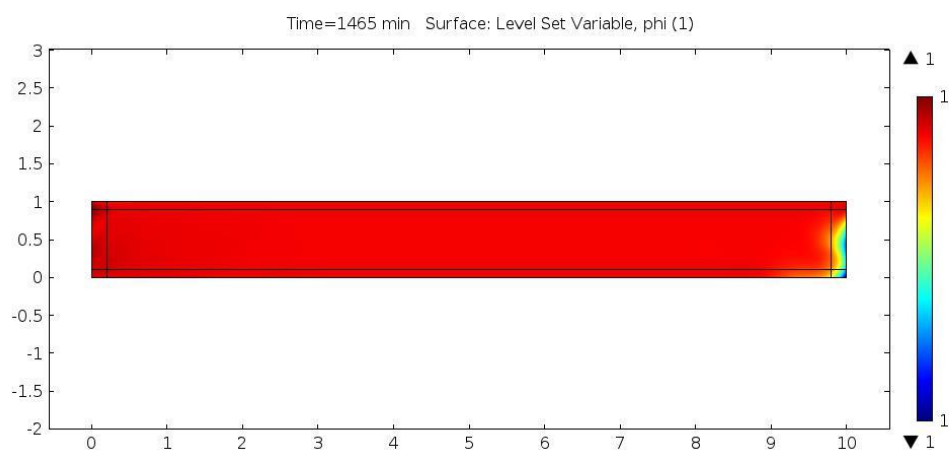
(e)

Figure 5.12 Simplified Filtration Model Flow Front tracking Results t=1m (a), =10m (b), t=400m (c), t=1000m (d), t=1465m (e)

It is crucial to obtain a homogeneous material to provide desired mechanical properties, so it is essential to provide same concentration value at whole preform. It is observed that concentration value is not homogeneous through the material when the front flow reaches to the outlet. In Figure 5.12 it is indicated that at time 1465-minute front flow reaches to the outlet but it can be observed that although concentration value is expected to be 30% through the whole geometry nearly, it is found out that 30% particle concentration reaches nearly half of the geometry and cannot catch up with the speed of flow (Figure 5.13).
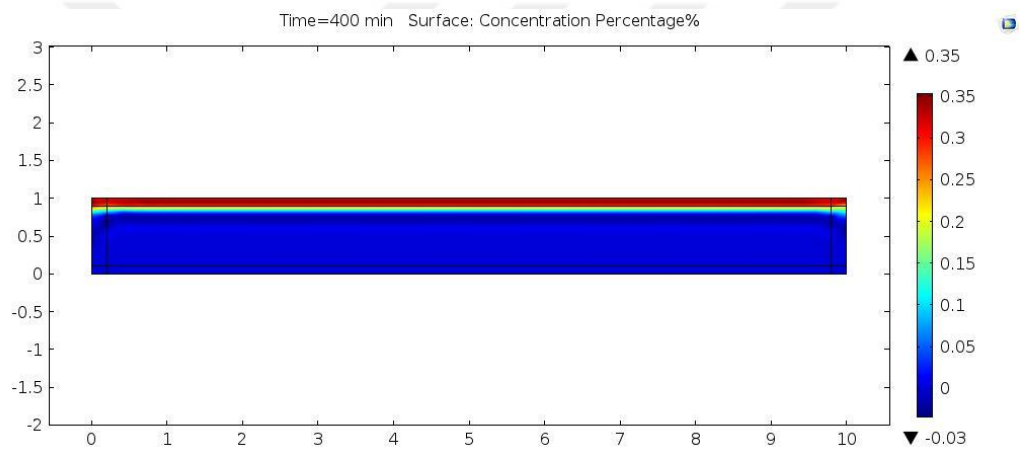
(a)
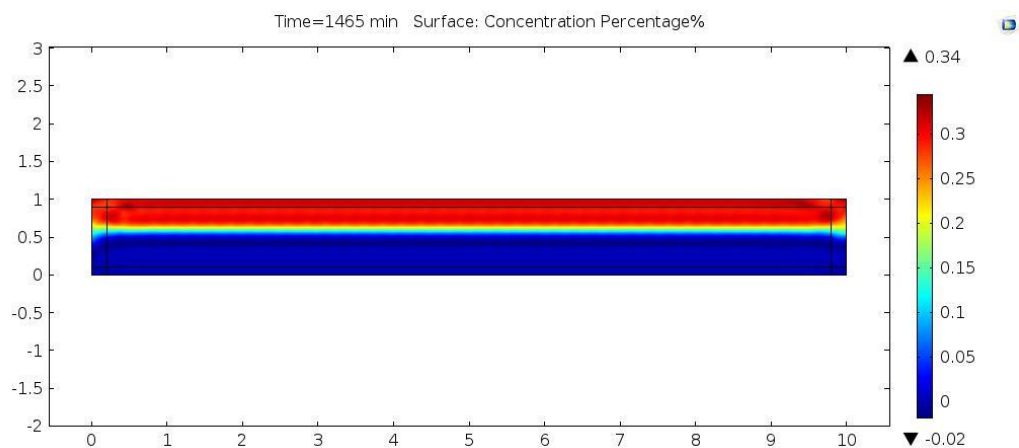
(b)

Figure 5.13 Concentration Percentages at t=400m (a), t=1465m(b)

However, when the front flow reaches to end, concentration value decreases dramatically after the half of the flow path (Figure 5.14) due to particle filtration, so until minute 6000 a partially unsaturated flow is present, which means flow must be continued until particle concentration reaches the desired value. So filling process should be continued to get more homogeneity through the material which can be analyzed from Figure 5.14. Also, it can be interpreted that particle filtration results in an exponential increase of homogeneous filling time.
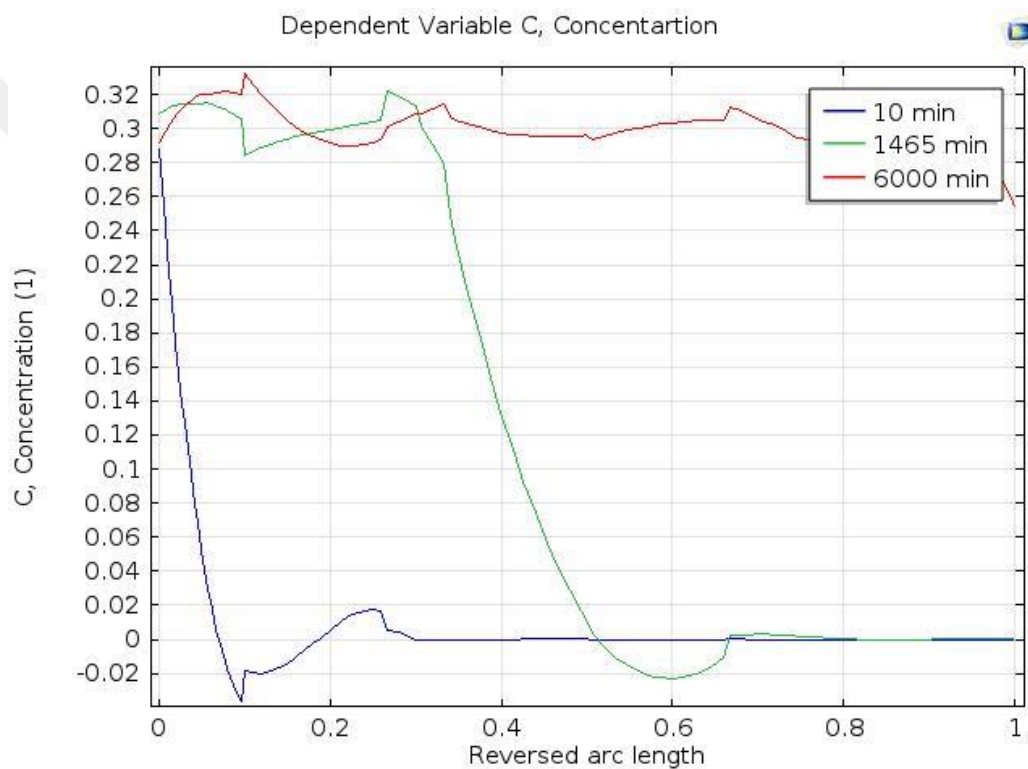
Figure 5.14 Concentration Values Through the Preform at t=10m, t=1465m, and t=6000m

Additionally, this advancing concentration profile is an indication of filtration profile which slows down particle concentration increment. So, it is expected that retention (σ) profile gets the highest value as it gets closer to the inlet and decreases through the outlet. This necessity is obtained with retention values through path for all time steps in Figure 5.15.
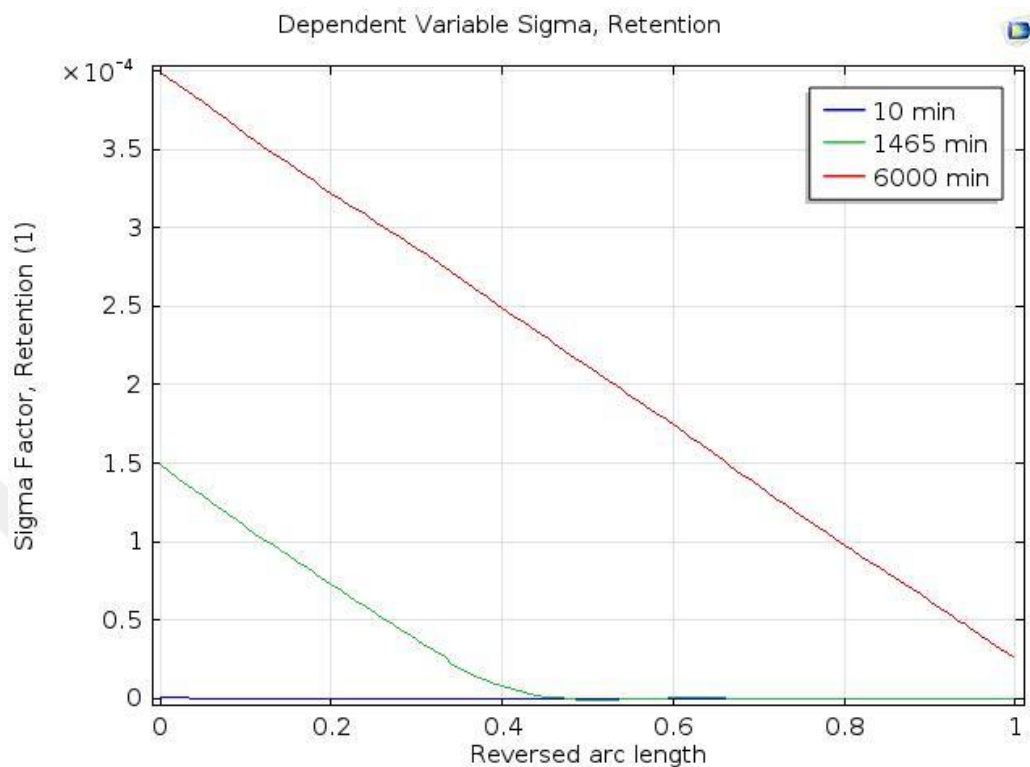
Figure 5.15 Retention Values Through Flow Path at t=10m, t=1465m, and t=6000m

Another parameter, total particle value distribution is a way of check the correctness of mass conservation. Total particle value must be around a constant value until the border until where the maximum concentration value 30% is satisfied. In Figure 5.16 it is indicated that t=1465m flow front reaches to end of the geometry, but concentration value does not reach to 30% (full concentration of particles in the resin). Therefore, total particle value starts to drop with concentration value. Homogeneous particle distribution with 30% concentration was obtained at Time=6000 m and also total particle value was much more stable through whole geometry.
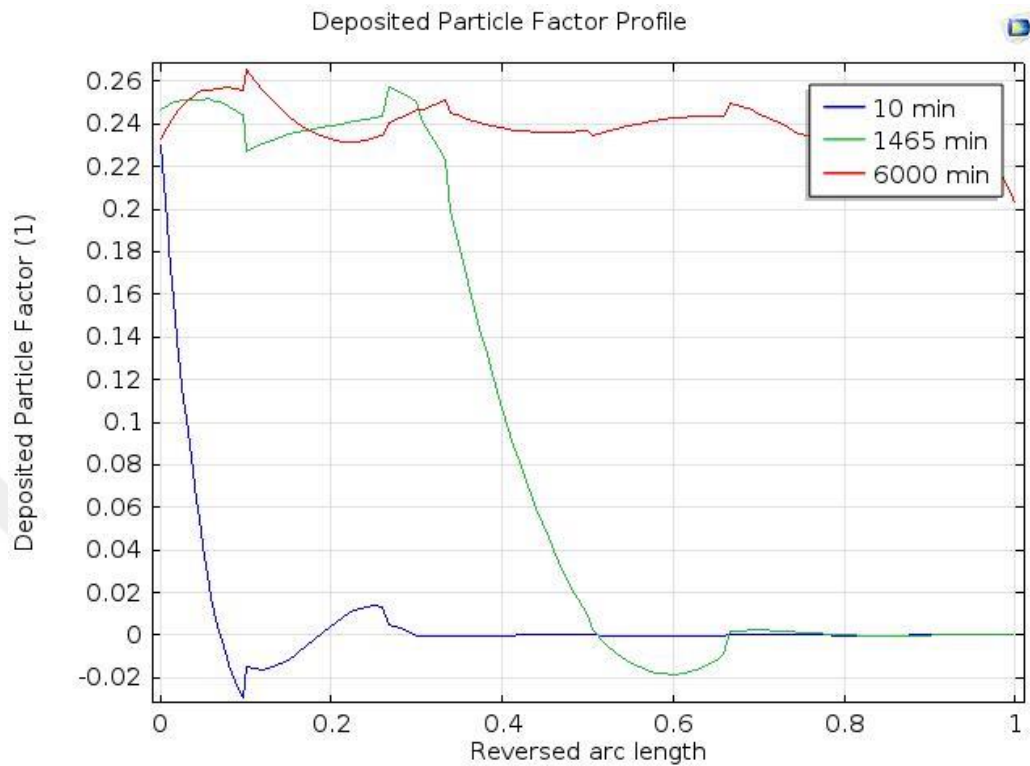
Figure 5.16 Total Particle Value Profiles

The whole study shows that CRTM logic works with RTM process but reaching time to desired concentration value is independent of superficial filling time. Therefore, perfect filling time must be determined by numeric simulations and be verified with experimental results.

Chapter 6

6 Conclusion & Future Work

Consequently, hybrid composite production process involves various physics and in that thesis, macro-level flow is considered instead of meso-level and micro-level flows in porous media. In literature, experiments showed that macro-level flow is a creeping flow. Also, considered fluid was a resin with nanoparticles which would be filtered by porous media. Therefore, a mathematical model was constructed with Darcy's Law, momentum and filtration equations for resin flow in porous media. In numerical model constructed mathematical model equations were used to define the physics and simulations constructed over that mathematical model. Also, a flow tracking method was needed, and Level Set Method was used due to its' relatively basic math.

Numeric simulation tests were started by verifying the compatibility of Level Set Method with the analytical solution. After obtaining compatibility, the filling process for both parallel 2-layer and 6-layer geometries consisting highly differing permeable 2 materials were analyzed. It is found out that traditional RTM process, in which filling process is from side boundary, is not capable of filling porous media as homogeneous due to forming voids during the filling process. It was observed that flow could not advance through high permeable layer when inlet boundary is perpendicular to the orientation of layers. In order to get a fully filled structure CRTM filling logic is embedded to traditional RTM production method and filling boundary was moved to the top of the geometry.

By this way, inlet boundary became parallel to the layer orientation. By applying CRTM logic to traditional RTM process layer by layer filling sequence was constructed. By that, we were satisfied with obtaining a geometry without void. Next step was inputting filtration model to simulation, and it is found out that filtration phenomenon increase in filling time dramatically. The process time of the front flow pass through the outlet does not equal to the time when a homogeneous particle distribution is obtained. In simulations, even particle distribution through the geometry took much more time than the time at which resin passes through the part. Excess resin injection is an essential economical problem to be solved via shortening the filling time which is expected to be solved via applying positive pressure from outlet region. Additionally, longer filling times can cause crosslinking during injection and so deviations from desired mechanical and physical properties. Another way of getting faster flow is decreasing viscosity with higher temperature unfortunately, gelatinization becomes an issue to consider. Therefore, filling time, viscosity, crosslinking mechanics and gelatinization relationship are linked which must be kept in mind while figuring out advance solution for that system.

In order to bring perfection to this study; some improvements may be researched in terms of numeric analysis, mathematical model and also, experimental analysis for validation of model and simulation should be conducted as future work. For numeric model improvement, different front flow tracking methods such as; Volume of Fraction and Phase Field Methods may be implemented to numeric model and comprised to determine the most consistent one. Additionally, the mathematical model may be perfected by Brinkman, and Forcheimmer's equations extended Darcy's Law. Some other physics such as; micro level-flow and meso-level-flow occurring during the process will be analyzed.

Also, experimental validation of the simulation can be done. Experimental tests would provide practical informations about the relationship between resin and mold temperature (resin visvosity), filling time, gelatinization and cross linking rate. Mechanical characterizations of the produced specimen would be performed

with SEM outputs and mechanical tests. SEM results would provide us particle distribution profile of composite material specimen and so homogeneity of particle distribution. Finally, this method should be analyzed under cost and time-saving subjects, when it is used by aviation and automotive industry.

REFERENCES

[1]Hashin Z. Analysis of Composite Materials—A Survey. J Appl Mech 1983;50:481. doi:10.1115/1.3167081.

[2]   Simacek P, Advani SG, Iobst SA. Modeling Flow in Compression Resin Transfer Molding for Manufacturing of Complex Lightweight High-Performance Automotive Parts. J Compos Mater 2008;42:2523–45. doi:10.1177/0021998308096320.

[3]   Carvalho LH, Canedo EL, NETO SRF. Moisture Transport Process in Vegetable Fiber Composites: Theory and Analysis for Technological Applications. Ind Technol Appl Transp Pororus Mater 2013;36. doi:10.1007/978-3-642-37469-2.

[4]   Agarwal BD, Broutman LJ, Chandrashekhara K. Analysis and Performance of Fiber Composites. 2006.

[5]   Campbell FC. Introduction to Composite Materials. Struct Compos Mater 2010:1–29. doi:10.1017/CBO9781107415324.004.

[6]   Krenkel W, Langhof N. Proceedings of the IV Advanced Ceramics and Applications Conference. Proc. IV Adv. Ceram. Appl. Conf., Atlantis Press and the author(s); 2017. doi:10.2991/978-94-6239-213-7.

[7]   Wang Z, Liang Z, Wang B, Zhang C, Kramer L. Processing and property investigation of single-walled carbon nanotube (SWNT) buckypaper/epoxy resin matrix nanocomposites. Compos Part A Appl Sci Manuf 2004;35:1225–123. doi:10.1016/j.compositesa.2003.09.029.

[8]   Safadi B, Andrews R, Grulke EA. Multiwalled carbon nanotube polymer composites: Synthesis and characterization of thin films. J Appl Polym Sci 2002;84:2660–9. doi:10.1002/app.10436.

[9]   Yum SH, Lee W Il, Kim SM. Particle filtration and distribution during the liquid composite molding process for manufacturing particles containing composite materials. Compos Part A Appl Sci Manuf 2016;90:330–9. doi:10.1016/j.compositesa.2016.07.016.

[10]   Fu SY, Lauke B, Mäder E, Yue CY, Hu X. Tensile properties of short-glass-fiber- and short-carbon-fiber-reinforced polypropylene composites. Compos Part A Appl Sci Manuf 2000;31:1117–25. doi:10.1016/S1359-835X(00)00068-3.

[11]   Mishra S, Mohanty AK, Drzal LT, Misra M, Parija S, Nayak SK, et al. Studies on mechanical performance of biofibre/glass reinforced polyester hybrid composites. Compos Sci Technol 2003;63:1377–85. doi:10.1016/S0266-3538(03)00084-8.

[12]   Dyer SR, Lassila LVJ, Jokinen M, Vallittu PK. Effect of fiber position and orientation on fracture load of fiber-reinforced composite. Dent Mater 2004;20:947–55. doi:10.1016/j.dental.2003.12.003.

[13]   Jacob M, Thomas S, Varughese KT. Mechanical properties of sisal/oil palm hybrid fiber reinforced natural rubber composites. Compos Sci Technol 2004;64:955–65. doi:10.1016/S0266-3538(03)00261-6.

[14]   Laurenzi S, Marchetti M. Advanced Composite Materials by Resin Transfer Molding for Aerospace Applications. Compos Their Prop

2012:197–226. doi:10.5772/2816.

[15] Thwe MM, Liao K. Effects of environmental aging on the mechanical properties of bamboo-glass fiber reinforced polymer matrix hybrid composites. Compos - Part A Appl Sci Manuf 2002;33:43–52. doi:10.1016/S1359-835X(01)00071-9.

[16] Prabhakaran RTD, Andersen TL, Markussen CM, Madsen B, Lilholt H. Tensile and Compression Properties of Hybrid Composites - A Comparative Study. 19th Int. Conf. Compos. Mater. (ICCM 19), 2013, p. 1029–35.

[17] Reia Da Costa EF, Skordos AA, Partridge IK, Rezai A. RTM processing and electrical performance of carbon nanotube modified epoxy/fibre composites. Compos Part A Appl Sci Manuf 2012;43:593–602. doi:10.1016/j.compositesa.2011.12.019.

[18] Lee GW, Park M, Kim J, Lee JI, Yoon HG. Enhanced thermal conductivity of polymer composites filled with hybrid filler. Compos Part A Appl Sci Manuf 2006;37:727–34. doi:10.1016/j.compositesa.2005.07.006.

[19] Porfiri M, Gupta N. Effect of volume fraction and wall thickness on the elastic properties of hollow particle filled composites. Compos Part B Eng 2009;40:166–73. doi:10.1016/j.compositesb.2008.09.002.

[20] Chisholm N, Mahfuz H, Rangari VK, Ashfaq A, Jeelani S. Fabrication and mechanical characterization of carbon/SiC-epoxy nanocomposites. Compos Struct 2005;67:115–24. doi:10.1016/j.compstruct.2004.01.010.

[21] Cho J, Joshi MS, Sun CT. Effect of inclusion size on mechanical properties of polymeric composites with micro and nano particles. Compos Sci Technol 2006;66:1941–52. doi:10.1016/j.compscitech.2005.12.028.

[22] Uddin MF, Sun CT, Introduction I. Polymer Nanocomposites 2001;804:1–13. doi:10.1021/bk-2002-0804.

[23] Liu H, Webster TJ. Mechanical properties of dispersed ceramic nanoparticles in polymer composites for orthopedic applications. Int J Nanomedicine 2010;5:299–313. doi:10.2147/IJN.S9882.

[24] Tanoğlu M, Seyhan AT. Compressive mechanical behaviour of E-glass/polyester composite laminates tailored with a thermoplastic preforming binder. Mater Sci Eng A 2003;363:335–44. doi:10.1016/j.msea.2003.08.005.

[25] Kang MK, Lee WI, Hahn HT. Analysis of vacuum bag resin transfer molding process. Compos - Part A Appl Sci Manuf 2001;32:1553–60. doi:10.1016/S1359-835X(01)00012-4.

[26] Trochu F, Ruiz E, Achim V, Soukane S. Advanced numerical simulation of liquid composite molding for process analysis and optimization. Compos. Part A Appl. Sci. Manuf., vol. 37, 2006, p. 890–902. doi:10.1016/j.compositesa.2005.06.003.

[27] Masoodi R, Pillai KM, Grahl N, Tan H. Journal of Reinforced Plastics and Composites. Reinf Plast Compos 2012;31:363–78. doi:10.1177/0731684412438629.

[28] Bakshi SR, Lahiri D, Agarwal A. Carbon nanotube reinforced metal matrix composites - a review. Int Mater Rev 2010;55:41–64.

doi:10.1179/095066009X12572530170543.

[29]   Gibou F. Frederic Gibou - Research 2014.

[30]   Kendall KN, Rudd CD. Flow and cure phenomena in liquid composite molding. Polym Compos 1994;15:334–48. doi:10.1002/pc.750150504.

[31]   Ruiz E, Achim V, Soukane S, Trochu F, Bréard J. Optimization of injection flow rate to minimize micro/macro-voids formation in resin transfer molded composites. Compos Sci Technol 2006. doi:10.1016/j.compscitech.2005.06.013.

[32]   Gauvin R, Chibani M, Lafontaine P. The Modeling of Pressure Distribution in Resin Transfer Molding. J Reinf Plast Compos 1987;6:367–77. doi:10.1177/073168448700600406.

[33]   Shojaei A. Numerical simulation of three-dimensional flow and analysis of filling process in compression resin transfer moulding. Compos Part A Appl Sci Manuf 2006;37:1434–50. doi:10.1016/j.compositesa.2005.06.021.

[34]   Olivero KA, Hamidi YK, Aktas L, Altan MC. Effect of Preform Thickness and Volume Fraction on Injection Pressure and Mechanical Properties of Resin Transfer Molded Composites. J Compos Mater 2004;38:937–57. doi:10.1177/0021998304040562.

[35]   Mamoune a., Saouab a., Park CH. Simple Models of CRTM Process. Int J Mater Form 2008;1:911–4. doi:10.1007/s12289-008-0244-4.

[36]   Merotte J, Simacek P, Advani SG. Resin flow analysis with fiber preform deformation in through thickness direction during Compression Resin Transfer Molding. Compos Part A Appl Sci Manuf 2010;41:881–7. doi:10.1016/j.compositesa.2010.03.001.

[37]   Hwang WR, Advani SG, Walsh S. Direct simulations of particle deposition and filtration in dual-scale porous media. Compos Part A Appl Sci Manuf 2011;42:1344–52. doi:10.1016/j.compositesa.2011.05.017.

[38]   Chohra M, Advani SG, Gokce A, Yarlagadda S. Modeling of Filtration Through Multiple Layers of Dual Scale Fibrous Porous Media *. Polymer (Guildf) 2006. doi:10.1002/pc.

[39]   Han K, Jiang S, Zhang C, Wang B. Flow modeling and simulation of SCRIMP for composites manufacturing. Compos Part A Appl Sci Manuf 2000;31:79–86. doi:10.1016/S1359-835X(99)00053-6.

[40]   Boh JW, Louca LA, Choo YS, Mouring SE. Damage modelling of SCRIMP woven roving laminated beams subjected to transverse shear. Compos Part B Eng 2005;36:427–38. doi:10.1016/j.compositesb.2005.01.001.

[41]   Do people have to buy license for scrimp(Seemann composite resin infusion molding process)? - Quora n.d.

[42]   Rooney M, Murray GM, Roberts JC, Romenesko BM. Advanced Materials : Challenges and Opportunities. Johns Hopkins Apl Tech Dig 2015;21:516–26.

[43]   Erdal M, Guceri SI, Danforth SC. Impregnation Molding of Particle-Filled Preceramic Polymers: Process Modeling. J Am Ceram Soc 1999;82:2017–28. doi:10.1111/j.1151-2916.1999.tb02034.x.

[44] Lefevre D, Comas-Cardona S, Binetruy C, Krawczak P. Coupling filtration and flow during liquid composite molding: Experimental investigation and simulation. Compos Sci Technol 2009;69:2127–34. doi:10.1016/j.compscitech.2009.05.008.

[45] Dimitrovová Z. Finite element modeling of the resin transfer molding process based on homogenization techniques. Comput Struct 2000;76:379–97. doi:10.1016/S0045-7949(99)00174-1.

[46] Lin MYY, Murphy MJJ, Hahn HTT. Resin transfer molding process optimization. Compos Part A Appl Sci Manuf 2000;31:361–71. doi:10.1016/S1359-835X(99)00054-8.

[47] Trochu F, Gauvin R, Gao DM. Numerical Analysis of the Resin Transfer Molding Process by the Finite Element Method. Adv Polym Technol 1993;12:329–42.

[48] Bianco C, Tosco T, Sethi R. A 3-dimensional micro- and nanoparticle transport and filtration model (MNM3D) applied to the migration of carbon-based nanomaterials in porous media. J Contam Hydrol 2016;193:10–20. doi:10.1016/j.jconhyd.2016.08.006.

[49] Bréard J, Henzel Y, Trochu F, Gauvin R. Analysis of dynamic flows through porou-s media. Part I: Comparison between saturated and unsaturated flows in fibrous reinforcements. Polym Compos 2003;24:391–408. doi:10.1002/pc.10038.

[50] Mahale AD, Prud'Homme RK, Rebenfeld L. Quantitative measurement of voids formed during liquid impregnation of nonwoven multifilament glass networks using an optical visualization technique. Polym Eng Sci 1992;32:319–26. doi:10.1002/pen.760320504.

[51] Patel N, Lee LJ. Modeling of void formation and removal in liquid composite molding. Part II: Model development and implementation. Polym Compos 1996;17:104–14. doi:10.1002/pc.10595.

[52] Varna J, Joffe R, Berglund LA, Lundström TS. Effect of voids on failure mechanisms in RTM laminates. Compos Sci Technol 1995;53:241–9. doi:10.1016/0266-3538(95)00024-0.

[53] Goodwin AA, Howe CA PR. VOLUME IV COMPOSITES PROCESSING Editor. Compos Process Microstruct 1997;IV.

[54] Hanspal NS, Waghode AN, Nassehi V, Wakeman RJ. Development of a predictive mathematical model for coupled stokes/Darcy flows in cross-flow membrane filtration. Chem Eng J 2009;149:132–42. doi:10.1016/j.cej.2008.10.012.

[55] Lefevre D, Comas-Cardona S, Binétruy C, Krawczak P. Modelling the flow of particle-filled resin through a fibrous preform in liquid composite molding technologies. Compos Part A Appl Sci Manuf 2007. doi:10.1016/j.compositesa.2007.06.008.

[56] Vengimalla R, Chase GG, Ramarao B V. Modeling of filler retention in compressible fibrous media. Sep Purif Technol 1999;15:153–61. doi:10.1016/S1383-5866(98)00092-6.

[57] Metzner AB. Rheology of Suspensions in Polymeric Liquids. J Rheol (N Y N Y) 1985;29:739–75. doi:10.1122/1.549808.

[58] Zhou F, Kuentzer N, Simacek P, Advani SG, Walsh S. Analytic characterization of the permeability of dual-scale fibrous porous media. Compos Sci Technol 2006;66:2795–803. doi:10.1016/j.compscitech.2006.02.025.

[59] Herzig M Leclerc P Le Goff PD. Applicdtion to Deep Filtrdtion. Ind Eng Chem 1970;62:8–34.

[60] Carman P. Fluid flow through granular beds. Trans Inst Chem Eng 1937;15:150–66. doi:10.1016/S0263-8762(97)80003-2.

[61] Sacramento RN, Yang Y, You Z, Waldmann A, Martins AL, Vaz ASL, et al. Deep bed and cake filtration of two-size particle suspension in porous media. J Pet Sci Eng 2015. doi:10.1016/j.petrol.2014.12.001.

[62] Lekakou C, Bader MG. Mathematical modelling of macro- and micro-infiltration in resin transfer moulding (RTM). Compos Part A Appl Sci Manuf 1998;29:29–37. doi:10.1016/S1359-835X(97)00030-4.

[63] Coulter JP, Guceri S. Resin impregnation during composites manufacturing: Theory and experimentation. Compos Sci Technol 1989;35:317–30. doi:10.1016/0266-3538(89)90055-9.

[64] Ngo ND, Tamma KK. Microscale permeability predictions of porous fibrous media. Int J Heat Mass Transf 2001;44:3135–45. doi:10.1016/S0017-9310(00)00335-5.

[65] Kundu P, Kumar V, Mishra IM. Experimental and numerical investigation of fluid flow hydrodynamics in porous media: Characterization of pre-Darcy, Darcy and non-Darcy flow regimes. Powder Technol 2016;303:278–91. doi:10.1016/j.powtec.2016.09.037.

[66] Silva RA, Assato M, de Lemos MJS. Mathematical modeling and numerical results of power-law fluid flow over a finite porous medium. Int J Therm Sci 2016;100:126–37. doi:10.1016/j.ijthermalsci.2015.09.019.

[67] FIRDAOUSS M, GUERMOND J-L, LE QUÉRÉ P. Nonlinear corrections to Darcy's law at low Reynolds numbers. J Fluid Mech 1997;343:S0022112097005843. doi:10.1017/S0022112097005843.

[68] Sobieski W, Trykozko A. DARCY'S AND FORCHHEIMER'S LAWS IN PRACTICE. PART 1. THE EXPERIMENT. Tech Sci 2014;17:321–35.

[69] De Schampheleire S, De Kerpel K, Ameel B, De Jaeger P, Bagci O, De Paepe M. A discussion on the interpretation of the darcy equation in case of open-cell metal foam based on numerical simulations. Materials (Basel) 2016;9. doi:10.3390/ma9060409.

[70] Sobieski W, Trykozko A. DARCY'S AND FORCHHEIMER'S LAWS IN PRACTICE. PART 2. THE NUMERICAL MODEL. Tech Sci 2014;17:337–50.

[71] Cogswell DA, Szulczewski ML. Simulation of incompressible two-phase flow in porous media with large timesteps. J Comput Phys 2017;345:856–65. doi:10.1016/j.jcp.2017.06.007.

[72] Bai R, Tien C. Effect of Deposition in Deep-Bed Filtration: Determination and Search of Rate Parameters. J Colloid Andnce 2000;231:299–311. doi:10.1006.

[73] Xu P, Yu B. Developing a new form of permeability and Kozeny–Carman

constant for homogeneous porous media by means of fractal geometry. Adv Water Resour 2008;31:74–81. doi:10.1016/j.advwatres.2007.06.003.

[74]   Ozgumus T, Mobedi M, Ozkol U. Determination of kozeny constant based on porosity and pore to throat size ratio in porous medium with rectangular rods. Eng Appl Comput Fluid Mech 2014;8:308–18. doi:10.1080/19942060.2014.11015516.

[75]   Hirt CW. Volume of Fluid (VOF) Method for the Dynamics of Free Boundaries * 1981;225:201–25.

[76]   FLUENT 6.3 User's Guide - 23.3.1 Overview and Limitations of the VOF Model n.d.

[77]   Chen F, Hagen H. A Survey of Interface Tracking Methods in Multi-phase Fluid Visualization. Vluds201011 2010:11–9. doi:10.4230/OASIcs.VLUDS.2010.11.

[78]   Mahady K, Afkhami S, Kondic L. A volume of fluid method for simulating fluid / fluid interfaces in contact with solid boundaries. J Comput Phys 2015;294:243–57. doi:10.1016/j.jcp.2015.03.051.

[79]   Cahn JW, Hilliard JE. Free Energy of a Nonuniform System. I. Interfacial Free Energy. J Chem Phys 1958;28:258–67. doi:10.1063/1.1744102.

[80]   Alpak FO, Riviere B, Frank F. A phase-field method for the direct simulation of two-phase flows in pore-scale media using a non-equilibrium wetting boundary condition. Comput Geosci 2016;20:881–908. doi:10.1007/s10596-015-9551-2.

[81]   Sethian JA, Smereka P. Level Set Methods for Fluid Interfaces. Annu Rev Fluid Mech 2003;35:341–72. doi:10.1146/annurev.fluid.35.101101.161105.

[82]   Osher S, Sethian JA. Fronts propagating with curvature-dependent speed: Algorithms based on Hamilton-Jacobi formulations. J Comput Phys 1988;79:12–49. doi:10.1016/0021-9991(88)90002-2.

[83]   Sethian JA. Level Set Techniques for Tracking Interfaces: Fast Algorithms, Multiple Regions, Grid Generation and Shape/Character Recognition. Proc Int Conf 1994.

[84]   Brock DC, Jr FMO. Flow Visualization of Viscous Fingering in Heterogeneous Porous Media. Soc Pet Eng Inc 1991:211–22.

[85]   Homsy. Viscous Fingering in. Ann Rev Fluid Mech 1987;19:271–311.